Alma Mater Studiorum – Università di Bologna

DOTTORATO DI RICERCA IN

SCIENZE BIOMEDICHE

Ciclo XXIX

Settore Concorsuale di afferenza: 05/E1
Settore Scientifico disciplinare: BIO/10

The role of the ATPase Inhibitor Protein, IF_1, in the regulation of both mitochondrial function and Ca^{2+} homeostasis in tumor cells

Presentata da: **Giulia Gorini**

Coordinatore Dottorato

Prof. Lucio Cocco

Relatore

Prof. Giancarlo Solaini

Correlatore

Prof.ssa Alessandra Baracca

Esame finale anno 2017

Index

1 INTRODUCTION

1.1 Mitochondria and cell metabolism

Mitochondria are important cytosolic organelles directly involved in the energy production in cells. Their inheritance is maternal and the theory by which they originated from symbiotic bacteria living in cells is almost fully accepted (1). Endosymbiotic theory states that ages ago mitochondria were free-living prokaryotes that became active organelles of eukaryotic cells. If initially accepted for the sole plant plastids, this theory was then considered valid for mitochondria as well (2), given the fact that either physiological or biochemical aspects of these organelles are similar to prokaryotic cells (3). Mitochondria coevolved with their host, the eukaryotic cell, such that the majority of mitochondrial proteins is encoded by the cell nucleus. They however are equipped with an own small DNA genome of 16 Kb which encodes for tRNAs, rRNAs and major proteins involved in oxidative phosphorylation (OXPHOS), an essential process for ATP (adenosine triphosphate) production in cells. Therefore, mitochondria are important bioenergetics factories critical for normal cell function and metabolism. For this reason, mitochondrial diseases in human cells can be dangerous, affecting many important tissues, such as nervous tissue, heart and muscle (4). The observation by Otto Warburg that cancers usually acquire the property of taking up and fermenting glucose to lactate in the presence of oxygen led him to propose that mitochondrial respiration defects are the underlying basis for aerobic glycolysis and cancer (5). Not all tumors, however, necessarily undergo aerobic glycolysis to rapidly produce the energy required for tumor growth and progression (6). A consistent amount of studies on different cancers has been conducted over the years and the current data seem to support the view that in order to favour the production of biomass, proliferating cells are commonly prone to satisfy the energy requirement utilizing substrates rather than completely oxidizing glucose (to CO_2 and H_2O). More precisely, only part (40 to 75%, (7)) of the cell need of ATP is obtained through the scarcely efficient catabolism of glucose to pyruvate/lactate in the cytoplasm and the rest of the ATP need is synthesized in the mitochondria through the tricarboxylic acid (TCA) cycle (one ATP produced each acetyl

moiety oxidized) and the associated oxidative phosphorylation that regenerates nicotinamide- and flavin-dinucleotides in their oxidized state (NAD^+ and FAD).

1.2 Mitochondrial structure

Adenosine triphosphate (ATP) is a highly energetic compound required for most cellular endergonic reactions and processes. Functional integrity of mitochondria is strictly dependent on the molecular dynamic that monitors their dimensions and structure. Several functions are indeed carried out by these organelles: ATP production via OXPHOS process, cell-signalling handling, apoptotic processes, cellular energetic state regulation, muscular contraction, ionic gradients maintenance through biological membranes. The wide range of mitochondrial functions is highly related to the mitochondrial structure. Electronic microscopy experiments showed that mitochondria are separated from the cytosol by a complex double-membrane architecture, consisting of an outer mitochondrial membrane (OMM) and an inner mitochondrial membrane (IMM) separated by an intermembrane space (IMS) a few nanometres thick (8) [Fig.1]. The IMM is extensively folded into the mitochondrial matrix (MM), forming a series of invaginations called *mitochondrial cristae* that enormously increase the IMM's surface, therefore increasing the number of sites on which OXPHOS reactions can take place (9). Small junctions of around 30 nm (*cristae junctions*) are able to directly connect the mitochondrial cristae to the IMS: it has been hypothesized that the cristae junctions may act as an effective barrier to reduce not only the free diffusion of protons from the MM to the IMS, but also to prevent the improper distribution of proteins between the two different sides of the IMM.

The IMM is impermeable to ions and polar molecules, an important characteristic that is fundamental for the maintenance of the proton electrochemical gradient created by the oxidative phosphorylation. Moreover, it is mainly composed of proteins rather than lipids since the mitochondrial complexes (normally associated in supercomplexes) responsible for the electron transport, are in here embedded. Another peculiarity is that the IMM doesn't contain cholesterol, a typical element of biological membranes, whereas it contains cardiolipin, a lipid that is usually present in bacterial membranes (10). As previously introduced, the IMM delimits the mitochondrial matrix (MM), characterized by a jellied consistency because of its high concentration in terms of proteins (around 500 mg/ml). The MM is the main site where the citric acid cycle (also known as tricarboxylic acid -TCA- cycle, or Kreb's cycle), and the fatty

acids oxidation take place and where mitochondrial DNA (mtDNA), ribosomes and the proteins involved in the apoptotic processes are carefully guarded (9).

The OMM which externally defines the organelle in the cytosol, has a thickness of around 5 nm and it is permeable to a lot of small molecules and ions, thanks to the fact that it owns large amounts of mitochondrial porin, also known as VDAC (Voltage-Dependent Anion Channel), an important protein of 32 kDa that is able to form channels on the OMM allowing the free diffusion of small molecules up to 5000 Da.

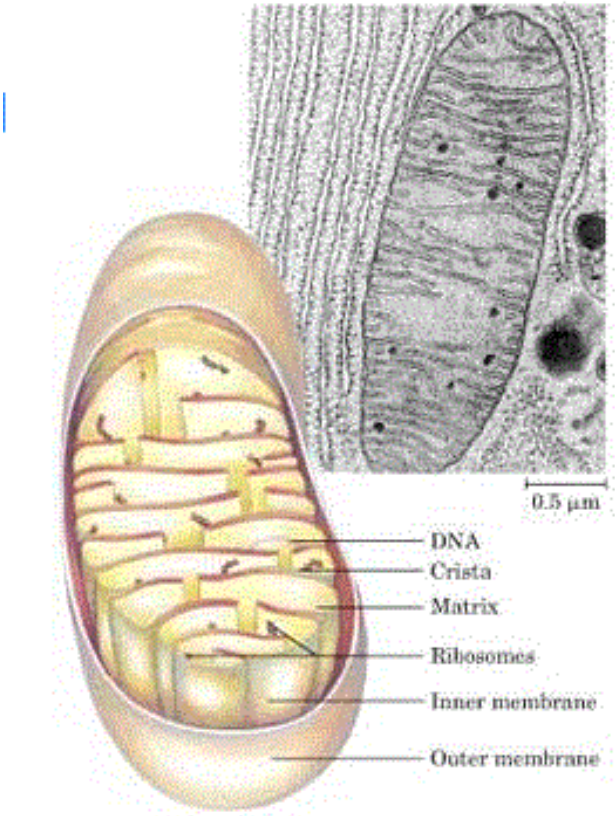

Fig. 1 Schematic representation of mitochondrial structure and electron microscopy of a mitochondrion showing the folding of the *cristae* into the mitochondrial matrix [Lehninger, D.L. Nelson and M.M. Cox, Principles of Biochemistry,3rd

As we can see in the picture [Fig.1], mitochondria look like small rods, with a diameter of around 0.3 µm and a length of around 1-6 µm. The number of mitochondria in one cell is variable according to the cellular type and to the cell's functional state. The mitochondrial life cycle starts with growth and division of pre-existing organelles (process known as *biogenesis*) and finishes with degradation of impaired or surplus organelles by a mechanism called *mitophagy*. In between, they undergo several cycles of fission and fusion that are fundamental for the generation

of heterogeneous mitochondria or interconnected mitochondrial networks, depending on the physiological state of the cell (11): the large mitochondrial networks that are generated by fusion are beneficial in metabolically active cells, in which they contribute towards the dissipation of energy (12). By contrast, in quiescent cells mitochondria are frequently present as numerous morphologically and functionally distinct small spheres or short rods. Mitochondrial fusion and fission are antagonistic activities that shape the mitochondrial compartment, and the consequent dynamic behaviour of mitochondria allows the cell to respond to its ever-changing physiological conditions (13). Thus, the rates of fusion and fission must be tightly controlled to keep the right balance required for the maintenance of mitochondrial morphology or to shift this balance to adapt the degree of mitochondrial interconnectivity to changing physiological conditions. As a matter of fact, fusion is involved in mitochondrial function and homeostasis maintenance whereas fission is responsible for the organelles division during mitosis, apoptotic factors release into the intermembrane space and damaged mitochondria turnover. Recent studies suggest that defects in the shape or distribution of mitochondria, possibly due to genetic mutations occurring in proteins related to fusion/fission balance (such as optic atrophy protein 1-OPA1, metalloendopeptidase OMA1, dynamin related protein 1-drp1, dynamin 1-dnm1), could be related to neurodegenerative diseases (e.g. Alzheimer's, Hungtington's and Parkinson's diseases) (14) (15) (16).

1.3 Mitochondrial genome

As mentioned, mitochondria are equipped with their own genome, the mitochondrial DNA (mtDNA), which is located in the MM. In mammalian cells, each organelle generally contains many identical copies of mtDNA. During its evolution into the present-day powerhouses of eukaryotic cells, the endosymbiont transferred many of its essential genes to the nuclear chromosomes. Nevertheless, the mitochondrion still carries hallmarks of its bacterial ancestor: for instance, it uses an *N*-formylmethionyl-tRNA (fMet-tRNA) as initiator of protein synthesis (17). Most mitochondrial proteins are in fact encoded by nuclear genes and imported into the organelles at a later time. To this end, at the time when they are synthesised, these proteins are composed of N-terminal pre-sequences of 20-50 amino which are able to drive them to a specific mitochondrial region according to the function they are meant to carry out (18).

The nucleotide sequence of the human mtDNA was the first documented complete sequence of a mitochondrial genome (19). Structure and gene organisation of mtDNA is highly conserved

among mammals. The mammalian mitochondrial genome is a closed-circular, double-stranded DNA molecule of 16569 pair bases [Fig. 2], encoding for 2 rRNAs and 22 tRNAs essential for the mitochondrial protein synthesis, and 13 polypeptides which constitute some of the enzyme complexes involved in the OXPHOS process. The OXPHOS proteins encoded by mtDNA are 7 subunits of the NADH-CoQ oxidoreductase (complex I), one subunit of the CoQ-cytocrome c reductase (complex III), 3 subunits of the cytocrome c oxidase (complex IV) and 2 subunits of the ATP synthase (ATPase 6 and ATPase 8) (20). The strands of the DNA duplex can be distinguished on the basis of G/T base composition which results in different buoyant densities of each strand ('heavy' and 'light') in denaturing caesium chloride gradients (21). Most information is encoded on the heavy (H) strand, with genes for 2 rRNAs, 14 tRNAs, and 12 polypeptides. The light (L) strand codes for 8 tRNAs and a single polypeptide. The replication of the H strand begins in a specific region of the mtDNA called *D-loop* where the promoters of both H and L strands are included. D-loop is a non-coding area of the mtDNA, a segment called control region, containing the binding sites for replication and transcription factors.

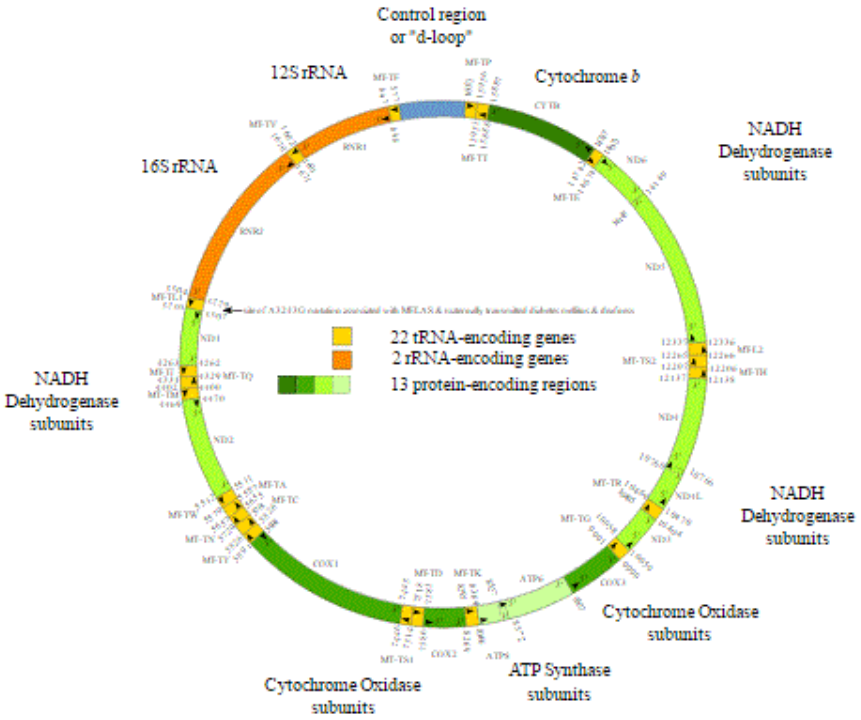

Fig. 2: Human mtDNA

Many differences with respect to the nuclear genome can be described: the genes lack introns and, except for one regulatory region, intergenetic sequences are absent or limited to a few

bases; both rRNA and tRNA molecules are unusually small; some of the protein genes are overlapping and, in many cases, part of the termination codons are not encoded but are generated post-transcriptionally by polyadenylation of the mRNAs (22). Another important difference is that mtDNA replication takes place independently from the cell cycle phases and occurs in all differentiated, even if non- proliferating, tissues. Finally, mtDNA reparation mechanisms are less efficient than the nuclear genome's ones explaining the high mutation rate occurring in mitochondria. The high mutation rate and the presence of several copies of mtDNA in a single mitochondrion are the reason why two different mutations are common: homoplasmy and heteroplasmy. The former is referred to a cell with a uniform pattern of mtDNA, either completely wild-type or completely mutant. The latter refers to a cell including mitochondria with both mutant and wild-type mtDNA. Therefore it is important to define the correlation between the mtDNA mutation degree and the altered phenotype entity in mitochondrial pathologies.

1.4 Mitochondrial functions

As introduced, energetic metabolism, apoptotic processes, reactive oxygen species (ROS) production and important cell-signalling pathways are regulated by mitochondria, which play a crucial role in the physiology of the cell. In particular, tricarboxylic acid cycle (TCA – Kreb's cycle) where Acetyl-CoA is completely oxidized to 2 CO_2 generates reducing agents, NADH and $FADH_2$, required to initiate the OXPHOS process. In addition, TCA cycle produces important precursors of anabolic pathways like gluconeogenesis, fatty acid, porphyrins and proteins biosynthesis. Moreover, fatty acid β-oxidation, urea cycle, amino acid oxidative deamination and membrane phospholipids synthesis take place in mitochondria (23). These organelles are indeed the most productive centres of ROS in the cell, since superoxide anion ($O_2^{\cdot -}$) is generated as a result of the electron transport dysfunction through the redox centres of the protein complexes (24). Cellular ROS concentration has to be strictly regulated: whereas low concentrations of ROS are able to modulate cell-signalling pathways, higher amounts of radicals could damage nucleic acids, lipids, enzymes, and trigger apoptotic processes. Another feature of mitochondria is the maintenance of Ca^{2+} homeostasis in the cell: this function is finely regulated by the close proximity of the organelles to the endoplasmic reticulum (ER), the main Ca^{2+} storage site in the cell, and by the numerous transporters wiped through the inner and the outer mitochondrial membranes. Finally, mitochondria are also responsible for the

thermogenesis phenomenon, essential in the brown adipose tissue to convert the energy derived from the OXPHOS into heat (25).

1.4.1 Electron transport chain and oxidative phosphorylation

Mitochondrial respiration is the main energy-yielding mechanism in aerobic eukaryotes. For this purpose, the evolution has created a well organised and efficient structure represented by the electron transport chain (ETC): it is composed of four protein complexes and two mobile transporters (coenzyme Q - CoQ, and cytocrome c - cyt c), most of which are embedded in the IMM. The protein complexes contain functional redox centres able to accept electrons from reduced donors and to release them to available acceptors, allowing their transport up to oxygen (O_2), which is the final acceptor of the chain [Fig. 3].

Complex I (also known as NADH/ubiquinone oxidoreductase, NADH-CoQ oxidoreductase, NADH dehydrogenase) directly receives electrons from nicotinamide adenine dinucleotide (NADH) generated by Kreb's cycle. It internally presents a flavoprotein associated to a flavin cofactor (FMN) able in fact to accept two electrons released by NADH. The electrons move from FMN, passing through iron-sulfur redox clusters, towards Coenzyme Q, a liposoluble ubiquinone, located inside of IMM. Ubiquinone's role is receiving electrons coming from both complex I and complex II, and to move them to complex III.

Complex II (succinate/CoQ reductase, succinate dehydrogenase) is the only TCA cycle enzyme located in the IMM. It is involved in both Kreb's cycle and OXPHOS. The conversion of succinate to fumarate, a reaction of citrate cycle, reduces FADH into $FADH_2$, from which electrons are taken and moved to complex II iron-sulfur centres and then to CoQ. The latter, thanks to its liposolubility, is able to diffuse through the membrane and transport these electrons up to complex III (cytocrome bc_1 complex or $CoQH_2$-cytocrome c reductase). Here the electrons promptly bind to the intermediate cytocrome c_1, which then transfers them directly to cyt c. Finally complex IV (cytocrome c oxidase - COX) captures the electrons from the cyt c and moves them to the final acceptor (O_2).

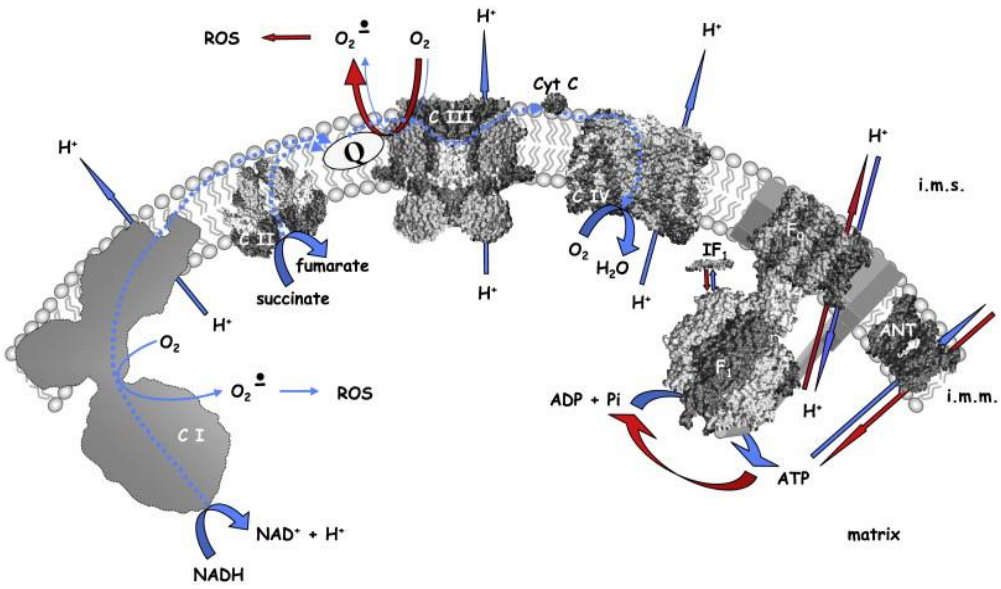

Fig 3. Electron transport chain and mitochondrial complexes. [Solaini G. et al., Biochimica et Biophysica Acta, 2010]

Thermodynamics studies demonstrated that all ETC-redox reactions are highly exergonic. The energy developed from the ETC reactions pushes the protons transport from the MM to the intracristae space, against concentration gradient. More precisely, this energy is sufficient to translocate 4 protons (H^+) from complex I, 4 H^+ from complex III, 2 H^+ from complex IV (26). Sir Peter Mitchell first explained the role played by the proton gradient, postulating the so called chemiosmotic theory (27). Protons movement from the mitochondrial matrix to the intermembrane space produces a transmembrane electrochemical potential ($\Delta\psi_m$), also called proton motive force ($\Delta\mu$), generated by the distribution of both electric charges ($\Delta\psi$) and chemical species (ΔpH) between the MM and the IMS. In particular, in the mitochondrial matrix $\Delta\psi_m$ is negative (around -150/180 mV) and it's used by the F_1F_O-ATPase to synthesise ATP from ADP + Pi. The IMS protons are in fact picked up by the enzyme to trigger a rotational catalysis responsible for ATP production. $\Delta\psi_m$ is therefore essential for the maintenance and control of the energetic state in the cell.

1.4.2 Importance of mitochondrial membrane potential

Several mitochondrial functions are strictly regulated by $\Delta\psi_m$, which is involved not only in the maintenance of the proton gradient required for ATP production, but also in ions homeostasis

control, metabolites transport, ROS production and cell death. For instance, it is the fuel for Ca^{2+} import into the mitochondrion under particular energy requests, such as during contraction in muscular cells (28). It has been also observed that in certain circumstances a high $\Delta\psi_m$ directly contributes to ROS production: an increased *delta* (Δ) of the mitochondrial transmembrane potential, principally associated to a decrease of ATP synthesis rate via OXPHOS which consequently causes a decrease of the electron transport rate through the IMM protein complexes, could determine a higher ability of the electrons to escape from the complexes redox centres and create reactive species in the presence of free O_2 (29).

Despite ATP synthesis handling is the most important aspect related to $\Delta\psi_m$, it is also essential for the preservation of mitochondrial morphology: an alteration of OPA1 (Optic Atrophy Protein 1) metabolism could induce a collapse of $\Delta\psi_m$, resulting in mitochondrial fragmentation, mitophagy activation pathways, mitochondrial permeability transition pore (mPTP) opening and apoptosis (30) (31).

The mitochondrial potential can also be altered by some classes of chemicals, such as uncouplers and ionophores, which can determine the complete dissipation of the proton gradient by forcing H^+ entrance in the MM. The uncouplers 2,4-dinitrophenol (DNP), carbonyl cyanide-4-(trifluoromethoxy) phenylhydrazone (FCCP), carbonyl cyanide m-chlorophenyl hydrazine (CCCP) are in fact able to bind and transport H^+ from the IMS to the MM, inducing the collapse of $\Delta\psi_m$ and nulling the proton gradient. Instead, ionophores like valinomycin, ionomycin or gramicidin create outright channels able to move many types of ions across the membrane. Finally, endogenous uncoupling proteins (UCPs) play an essential role in all animal tissues: they are capable of dissipating the proton gradient created by the ETC, like DNP, FCCP and CCCP do, to generate heat, when cells experience a decrease in temperature (32).

1.5 Mitochondrial F_1F_O-ATPase

The F_1F_O-ATPases (or ATP synthases) are multisubunit enzyme complexes of energetically active membranes in bacteria, mitochondria and chloroplasts. Mitochondrial ATP synthase uses the proton electrochemical gradient generated by the electron transport across the inner membrane (IMM) to produce the most important energetic source in the cell, adenosine triphosphate (ATP), from adenosine diphosphate (ADP) and inorganic phosphate (Pi). The enzyme consists of two major functional parts, a membrane-extrinsic F_1 portion, and a

membrane-intrinsic F_O (where "o" stands for "oligomycin") portion joined together by central and peripheral stalks. F_1 sector is the catalytic portion where ATP is synthesised, whereas F_O domain contains a motor, which generates rotation using the potential energy stored in the proton gradient. The rotational energy of the motor is then transmitted to the catalytic portion by the central stalk (33) [Fig. 4].

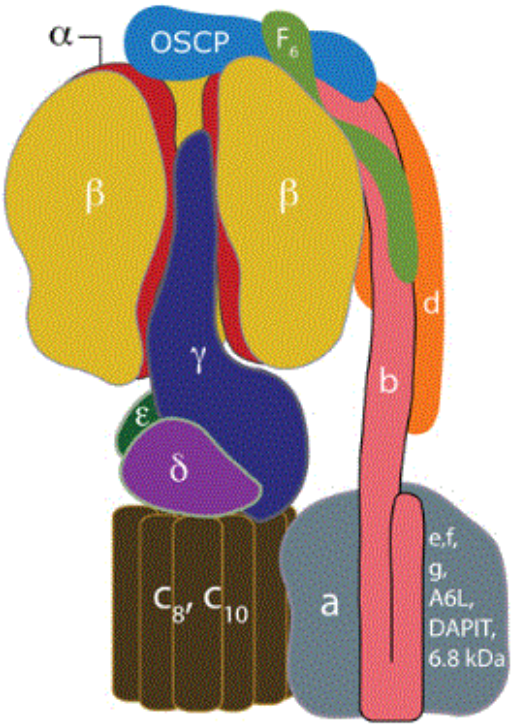

Fig.4. Schematic representation of mitochondrial F_1F_O-ATPase. [Walker, JE. The ATP synthase: the understood, the uncertain and the unknown. Keilin Memorial Lecture, 2012]

In mammals, F_O contains 8 *c-subunits*, each composed of two α-helix structures kept together by a loop region to form a ring inserted in the IMM, which is called *c-ring*. The c-ring is tightly in contact with the *a-subunit*, rich in basic-amino acids. The C-terminal α-helix of each c-subunit contains a carboxyl group, in the form of $–COO^-$, exposed on the external surface of the c-ring: as soon as H^+ ions cross the ring, they interact with $–COO^-$ groups neutralizing the negative charges and converting them to –COOH. Once neutralized, –COOH residues are able to pass through the hydrophobic environment of the phospholipid bilayer, generating the complete rotation of the c-ring. This mechanism allows the next $–COO^-$ group to be exposed inducing the second rotation. As c-ring rotations are triggered, –COOH residues are forced to

a second interaction with the a-subunit where the microenvironment furthers –COOH groups dissociation, making them available for the following ionic interactions. Protons are finally able to reach the MM passing through a second small channel which is part of the ring (33). The number of protons required to generate each 360° rotation of the c-ring corresponds to the number of c-subunits that form the ring.

In close proximity to a-subunit, a peripheral stalk extends from F_O domain to F_1 sector: it is composed of a single copy of OSCP (oligomycin-sensitivity conferring protein), b, d and F6 subunits (34). This structure facilitates a- and c- subunits contacts and makes F_1 sector more resistant during F_O rotation mechanism (35).

The F_1 domain of the ATP synthase is an assembly of 5 proteins: α, β, γ, δ, ε, with the stoichiometry of $\alpha_3\ \beta_3\ \gamma_1\ \delta_1\ \varepsilon_1$. The combined molecular mass of all these subunits is approximately 350 kDa. The three α- and the three β- form a spherical $\alpha_3\ \beta_3$ structure arranging in alternation around the γ subunit, completely enveloped in the $\alpha_3\ \beta_3$ domain. The γ subunit is fundamental to transfer the rotational energy coming from F_O sector to the catalytic subunits. Paul Boyer was the first scientist who proposed a mechanism that could explain the ATP synthesis driven by F_1 domain (36): according to his model, α-subunits bind one Mg^{2+} ion and one nucleotide, whereas each β-subunit is able to change its conformation 3 times giving rise to 3 different conformations, known as β_{TP}, β_{DP}, β_E, having different affinity to ADP and ATP. The synthesis starts when β_{DP} binds ADP and Pi, inducing a conformational change of β_{DP} site, which assumes β_{TP} configuration and promotes the conversion of ADP into ATP. Once ATP is produced, β_{TP} modifies its structure to β_E, characterized by a low affinity for ATP, consequently allowing its release in the MM [Fig.5].

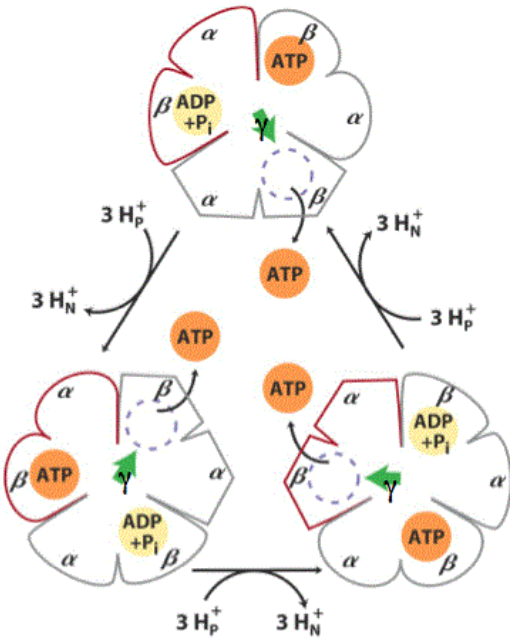

Fig.5. Conformational changes occurring in F_1 sector to synthetize ATP [Lehninger, D.L. Nelson and M.M. Cox, Principles of Biochemistry, 3rd edition 2000]

As widely explained in literature, mitochondrial ATP synthase is a reversible molecular motor, such that when $\Delta\psi_m$ is compromised, as it occurs when mitochondrial respiration is dramatically impaired, the enzyme is able to work in reverse hydrolysing cytosolic ATP to restore normal $\Delta\psi_m$ levels (37) (38). In this case, the F_1 sector directly picks up and binds the ATP molecules present in the MM and, thanks to F_O's ability to work in a counterclockwise direction, releases ADP and H^+ in the IMS, thus regenerating both proton gradient and $\Delta\psi_m$. What basically happens is that when hydrolysis is activated, ATP is bound to β_E site of the enzyme inducing the same conformational change occurring during ATP synthesis. How this happen is still under investigation: some investigators propose that β_{TP} is the site where ATP is hydrolysed, whereas some others say that this reaction occurs on the β_{DP} subunit (39). The second hypothesis has been so far considered the most reliable.

Despite a single enzymatic complex of ATP synthase is fully able to produce ATP, it has been proved that the enzyme normally organizes in dimers and oligomers rather than in single monomers. The association of two or more ATP synthases in oligomeric complexes is important for the stabilization of the enzyme and for the protection against mechanical insults during its catalytic activity. It has also been demonstrated that ATP synthase dimers intervene in cristae

remodelling and in the generation of areas in which protons are better rerouted for the ATP synthesis (40).

1.5.1 ATP synthase regulation

Under physiological conditions, ATP synthase activity is strictly regulated. Therefore, the electron transport across the complexes is finely controlled and directly related to ADP concentration in the physiological medium. When the metabolic state of the cell changes and a higher amount of ATP is requested, ADP concentration is increased and ATP synthesis rate becomes higher. This event is induced by an up-regulation of the Kreb's cycle, which consequently induces an increase in the dehydrogenases activation and NADH concentration (41).

ATP synthase's hydrolytic activity is carefully regulated as well, since physiological amounts of ATP are essential for cell life and survival. The uncontrolled and prolonged ATP consumption occurring when $\Delta\psi_m$ collapses, could provoke a complete deprivation of intracellular energy, which could lead to cell death. The most important regulator of this process is the ATP synthase Inhibitory Factor 1 (IF_1). Beyond the canonical and at this point accepted role of the protein in this function, it has been lately observed its involvement in the maintenance of mitochondrial morphology and network, and in carcinogenesis process, favouring tumor cells growth and proliferation.

1.6 The mitochondrial ATP synthase Inhibitory Factor 1: structure and binding to ATP synthase

As introduced above, ATP synthase activity needs to be strictly controlled. In animals and plants it is finely regulated by the endogenous, nuclear-encoded, ATP synthase Inhibitory Factor, IF_1, a small basic protein of 81-84 amino acids first discovered by Pullman and Monroy in 1963 (42). Its canonical function has been observed when the proton electrochemical gradient across the IMM is lost (during hypoxia/ischemia, as it occurs in tumors) or when IMM's integrity is compromised. In such condition, ATP synthase nanomotor is able to work in reverse hydrolysing cytosolic ATP to sustain $\Delta\psi_m$. In order to avoid the uncontrolled wasting of cellular ATP, IF_1, which is activated by a decrease of pH in the MM, binds to ATP synthase and blocks

the ATP consumption. In vitro, at a pH of 6.7 or below, this protein forms a 1:1 complex with either F_1 domain or with the intact ATP synthase (43). Once the electrochemical gradient is restored, IF_1 is released and ATP synthesis resumes.

It is encoded by the ATPIF1, a nuclear gene located in the chromosome 1, and it fulfils its function in MM. IF_1 is a small protein of around 10 kDa, well conserved among the species: as a matter of fact, human and bovine IF_1 proteins show up to 75% of similarity (44). The active bovine protein is a homodimer, where the C-terminals of the two α-helical monomers form an antiparallel coiled-coil. The protruding N-terminal regions represent the inhibitory domain of the protein, able to bind two F_1-ATPase moieties at the same time (45) [Fig.6]. At pH values of 8 and higher, dimers of IF_1 form dimers of dimers and more complexes aggregates, hiding the inhibitory domain of the protein and rendering it inactive. Disaggregation of these oligomers is thought to be managed by a His^{49} residue, which probably controls the pH-dependent interconversion between the inactive and active forms of the protein [Fig.7]

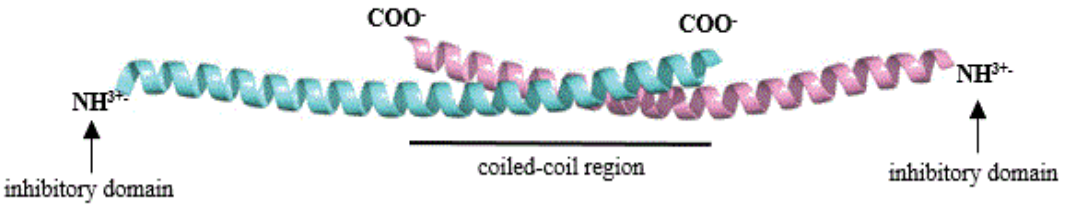

Fig. 6. Schematic representation of ATP synthase Inhibitory Factor 1 α-helices. [Walker JE. The ATP synthase: the understood. the uncertain. the unknown. Keilin Memorial Lecture. 2012]

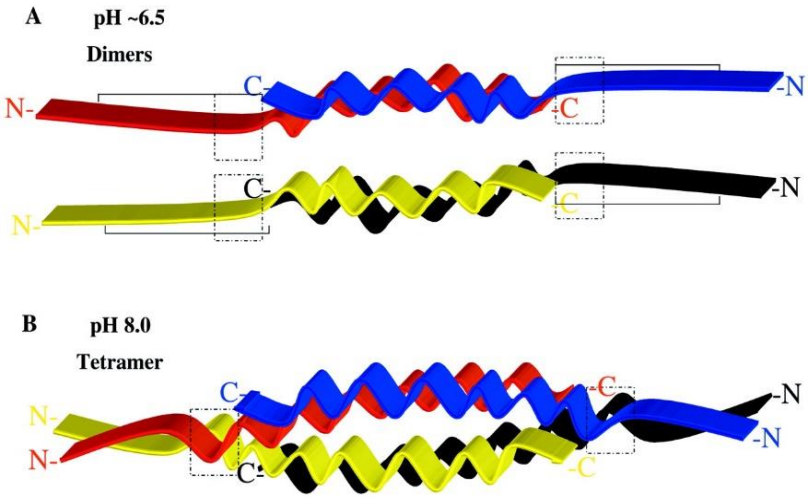

Fig. 7. Schematic drawing of the interconversion between dimers and tetramers of ATP synthase Inhibitory Factor 1. [Cabezòn et al., JBC, 2000]

More precisely, mature bovine IF_1 proteins are imported from the cytosol into the MM thanks to an N-terminal presequence of 25 amino acids. The inhibitory domain (ID) is located in the N-terminal region and confers IF_1 the ability to interact with the F_1 domain of the ATP synthase. A calmodulin-binding site has also been identified (46): it involves 33-42 residues and it's thought to be part of Ca^{2+} homeostasis regulation mechanism. This region is followed by a histidine-rich region (HRR), from 48 to 70 residues, implicated in the pH-sensitivity mechanism and hence in IF_1 activation process. IF_1 dimerization is controlled by the C-terminus of the protein (dimerization domain – DD), whereas its oligomerization is driven by the oligomerization domain (OD) hosted by the N-terminal region (47) [Fig. 8].

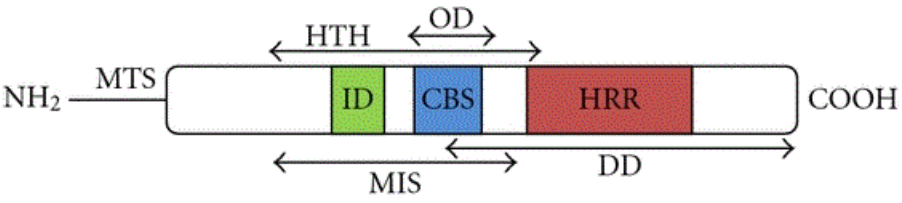

Fig. 8. Schematic representation of IF_1 domains. [Faccenda D., Campanella M., International Journal of Cell Biology, 2012]

In the bovine complex, IF_1 is inserted in a groove lined with α-helices in the C-terminal regions of α_{DP} and β_{DP} subunits of the enzyme, while its N-terminal region interacts with the coiled-coil α-helix of the γ-subunit extending to the central cavity of F_1 sector. Most of IF_1 residues are involved in hydrophobic interactions with the C-terminus of β_{DP} and β_{TP} subunits. In addition, more binding energy is provided by ionic interactions between IF_1 and F_1ATPase. Two possible molecular inhibition mechanisms have been proposed: according to the first one, IF_1 interacts with F_1 β-subunits preventing the release of hydrolysed ADP. The second theory states that once IF_1 is bound to the enzyme, ATP hydrolysis is prevented and ATP is promptly released (48). In any case, it is nowadays accepted that IF_1 selectively inhibits, through a non-competitive mechanism, the ATP-hydrolysing activity of the ATPsynthase without affecting the synthesis of ATP during oxidative phosphorylation.

Despite for a long time IF_1 activity has only been related to the inhibition of ATP hydrolysis in case of mitochondrial membrane impairment, in the last few years many research teams have shed light on the possible involvement of the inhibitor protein in the dimeric arrangement of the ATP synthase and in the mitochondrial cristae biogenesis and remodelling. Its importance wouldn't be related to the sole bioenergetics modulation, but it would also be connected to the maintenance of the proper mitochondrial morphology (40)(49).

1.6.1 Importance of IF_1 in tumors

As largely described, IF_1 directly affects the preservation of the cell energetic balance. Moreover, IF_1 may also be involved in the pre-conditioning process in heart, a phenomenon that could allow this tissue to better adapt and resist to various and brief ischemic insults: thanks to its direct interaction with the ATP synthase, IF_1 would be able to slow down the dissipation of ATP and thus to increase the time interval between the ischemic episode and the following reperfusion (50).

Since preliminary studies on IF_1 have been carried out mainly in primary cell lines, for the last few years the scientists have been trying to elucidate the role of IF_1 in tumor cells metabolism. Interestingly, it has been observed that it is in fact overexpressed in many human cancers, e.g. hepatocellular carcinoma, breast, lung carcinomas, colon carcinoma, cervical cancer and Yoshida's sarcoma (51) (52). Some studies have shown that IF_1- non expressing cells die more quickly if deprived of glucose and oxygen, a condition which normally occurs in specific tumor

areas. In addition, IF_1 could also participate in the activation of NfkB, an important promoter of cell proliferation and survival (53). The activation of this pathway has been associated to an increased superoxide radicals production. Nevertheless, contrasting data regarding ROS production modulation in the presence or absence of IF_1 are reported, keeping in mind that ROS can cause different effects on cells (54) according to the cell metabolic state, in particular its ROS/antioxidants balance. ROS can in fact interact with many genes and proteins involved either in cell proliferation (such as NfkB, AP-1) or in cell death mechanisms, which can also be prevented by IF_1.

Beyond this, electronic microscopy analysis have confirmed the possible involvement of IF_1 in the mitochondrial cristae stabilization in tumor cell lines: IF_1-expressing cells show in fact more organized and branched mitochondrial network and a higher number of cristae with respect to controls. Since an increasing number of studies seems to indicate that IF_1 could probably promote or stabilize dimeric forms of the ATP synthase, one might hypothesize that it also prevents mPTP opening and cyt c release, two important events preceding programmed cell death (55).

While some preliminary data proposed that IF_1 could further regulate the ATP synthase activity, by inhibiting ATP synthesis rate via OXPHOS and consequently inducing $\Delta\psi_m$ increase, it's now mostly accepted that IF_1-non expressing cells present higher $\Delta\psi_m$ (56) (57), associated to lower oxygen consumption rate. These results, sustained by further evidence, allowed to suppose that probably the inhibitor protein stimulates the OXPHOS process under normoxic physiological conditions.

1.6.2 IF_1 and the oligomeric organization of the ATP synthase

The role played by the inhibitor protein in the oligomeric organization of mitochondrial ATP synthase is still under debate: while some investigators firmly state that IF_1 is directly involved in the regulation of the oligomeric state of the enzyme, others say that ATP synthase oligomeric arrangement is independent from IF_1 presence or up-regulation. According to many researchers, IF_1 would directly contribute to ATP synthase dimerization by binding two F_1 portions at the same time (47) (58), thus promoting mitochondrial cristae formation and morphology and ultrastructure preservation (49). García and co-workers observed an increased dimer/monomer

ratio in rat liver and bovine heart ATP synthases when IF_1 expression increase was induced, whereas a decrease of the same ratio was detected when IF_1 was removed. On the other hand, some experiments carried out by Lippe's team in Udine (IT), would lead to conclude that in bovine heart mitochondria the dimeric organization of the enzyme is independent from IF_1 binding (59).

The mechanism by which IF_1 would be able to bind two different F_1 domains is shown in Fig. 9 and starts with the pathological collapse of the mitochondrial membrane potential and the consequent decrease of pH in the MM. In this condition, IF_1 active dimers adhere to the αβ interfaces of two different F_1 portions made available by two distinct ATP synthases, actively contributing to the dimer creation. By inducing the formation of dimers and even superior oligomers of the enzyme, the number of invaginations of the IMM into the MM significantly increases, leading to a more functional entrapment and distribution of protons in the close proximity of the enzymes. This mechanism has been explained by Strauss and co-workers, who demonstrated, by high resolution electronic microscopy, that ATP synthase's dimers tend to line up in *ribbons* that settle along the mitochondrial membrane. The dimer ribbons enforce a strong local curvature of the membrane, increasing the inner membrane's surface and generating areas of higher proton concentration where the membrane is sharply curved. ATP synthases would therefore benefit from an increased proton gradient increasing ATP synthesis efficiency (40) [Fig.10].

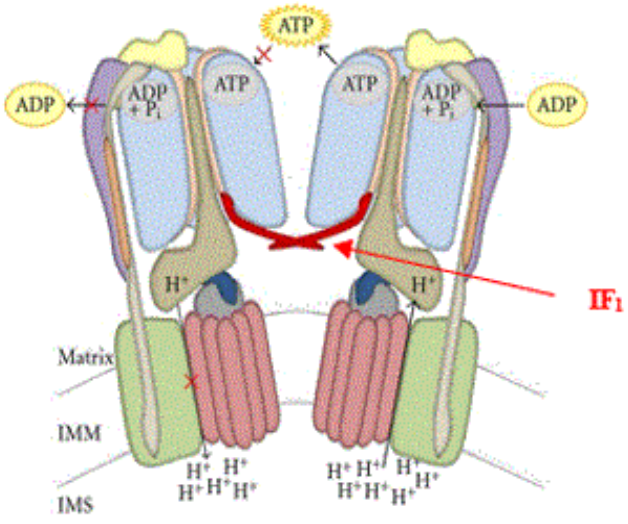

Fig.9. Schematic representation of the ATPP synthase dimer stabilized by IF_1. [Faccenda D., Campanella M., International Journal of Cell Biology, 2012]

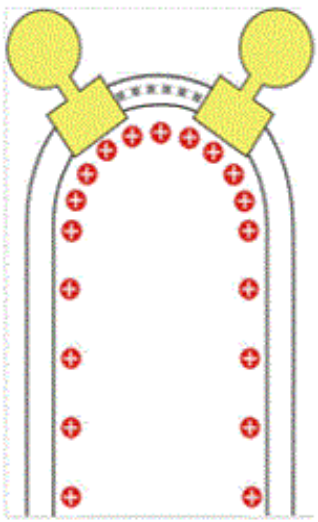

Fig.10. Schematic drawing of the proton traps created by membrane curvatures. [Strauss M. et al, EMBO J., 2008]

1.7 Hypoxia and ischemia in cancer

Cancer cells are characterized by a high proliferation rate. As a consequence, nutrients and oxygen trafficking in tumor cells is tremendously favoured in order to facilitate the tumor growth (60). High proliferating rate-cells extremely need quick ATP generation, high macromolecules biogenesis and accurate redox state control. In order to satisfy all these needs, tumor cells are characterized by significant alterations in the metabolism of all macromolecules (proteins, lipids, carbohydrates and nucleic acids). To be taken into consideration is that the growing tumor lives in a heterogeneous and dynamic microenvironment where nutrients and oxygen concentrations are continuously modified (61). In 1924, Otto Warburg conducted some studies on the altered use of glucose by cancer cells: according to his theory, they would increase glycolysis rate to satisfy the higher ATP request, consequently increasing lactate generation. In this scenario, OXPHOS process would be slowed down in spite of the normal concentration of oxygen (aerobic glycolysis) (62). This use of glucose by cancer cells may facilitate the quick tumor growth not only increasing the ATP production rate, but also increasing the availability of substrates, coming from either glycolysis or TCA or pentose phosphate pathway, necessary to induce new macromolecules biosynthesis. In addition, the consistent lactate accumulation would provoke an acidification of the cell environment, promoting invasiveness and tumor metastasis (63). In the last few years, Warburg's hypothesis has been largely questioned, since many studies have demonstrated the presence of still functional and working mitochondria in tumor cells. Indeed, many tumor cell lines, such as 143B and HeLa cells (64) (65), rely on OXPHOS to generate the ATP requested for tumor proliferation (6). The metabolic regulation occurring in cancers may be directly correlated with an actual decrease of oxygen, a condition which is called *hypoxia*. Nutrients and oxygen reach the solid tumor travelling across pre-existing and new-generated blood vessels, the latter created during a phenomenon called *angiogenesis*. When tumor is growing, the pre-existing vessels often undergo disruption and damage, whereas the new capillaries are characterized by structural abnormalities (66). These events, together with a possible reduction of the oxygen transport (as it happens during anaemia) or an increased oxygen consumption by cells, may contribute to the generation of hypoxic areas. Cells in the close proximity of the blood vessels are characterized by an oxygen concentration of around 2%, but, the larger the distance from the vessels is, the lower the oxygen tension becomes: cells 200 μm far from the capillary

endothelium may be even exposed to 0.2% oxygen concentration (severe hypoxia) (67). In order to allow the cell to face this event, many survival responses are activated. The first mechanism the cells adopt is the activation of the Hypoxia Inducible Factor 1 (HIF-1). HIF-1 was first identified in human cells as a regulator of erythropoietin, the hormone that controls red-cells production; vascular endothelial growth factor (VEGF), which stimulates angiogenesis; and glycolytic enzymes, which adapt cell metabolism to hypoxic conditions. HIF-1 is composed of a constitutively expressed HIF-1β subunit and an oxygen-regulated HIF-1α subunit. Under normoxic conditions (21% O_2), HIF-1α is hydroxylated by prolyl hydroxylase domain proteins (PHDs), that induce HIF-1α interaction with the von Hippel–Lindau (VHL) protein, the substrate-recognition subunit of an ubiquitin-protein ligase that targets HIF-1α for proteasomal degradation. Under hypoxic conditions, hydroxylation is inhibited and HIF-1α accumulates, binding HIF-1β and inducing the activation of hundreds of genes involved in cell adaptation to hypoxia (e.g. angiogenesis, erythropoiesis, glucose uptake, glycolysis, growth, invasiveness and metastasis transcription factors) [Fig. 11] (68). Together with the increase of the glycolysis efficiency and rate, HIF-1α activates the pyruvate-dehydrogenase kinase enzymatic complex (PDK), which inhibits pyruvate dehydrogenase (PD) activity. Following glycolysis, PD is responsible for the conversion of pyruvate into Acetyl-CoA essential to launch the TCA cycle and OXPHOS (69) (70).

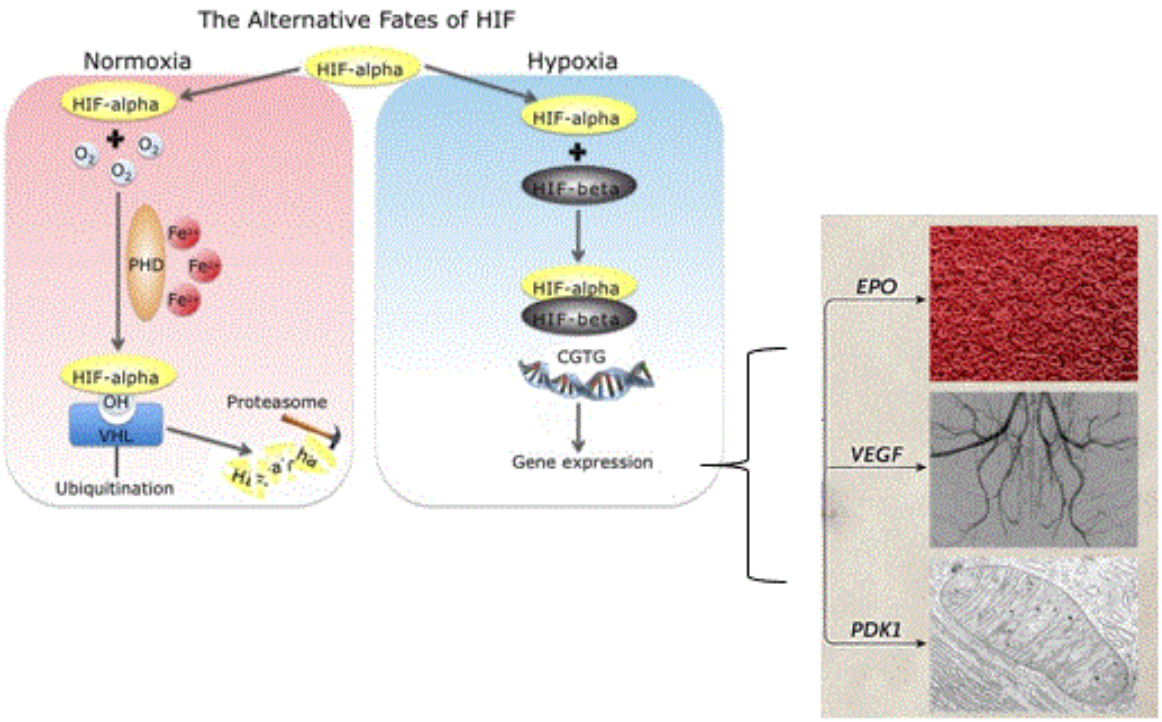

Fig. 11. The alternative fates of HIF and main adaptive mechanisms in hypoxia. [Semenza, G.L., The New England Journal of Medicine, 2011].

On the other hand, mitochondrial respiration rate is dramatically reduced by lack of oxygen itself, since this molecule is the final acceptor of the electron transport. If the oxygen deprivation is prolonged, the proton-motive force which drives ATP synthesis is lost and cells start to hydrolyse cytosolic ATP. As previously described, the reversal of the ATP synthase is fundamental to sustain the $\Delta\psi_m$ and cell homeostasis. However, if this process is uncontrolled, ATP availability could be compromised and in order to avoid this, IF_1 blocks ATP synthase's hydrolytic activity (71).

Yoshida and co-workers chemically mimicked the ischemic event in permanently IF_1-silenced HeLa cells by using the uncoupler CCCP (56): as already described, the uncouplers are hydrophobic weak acids which are able to load H^+ in the IMS, cross the IMM, and release them in the MM, dissipating the proton gradient. In such situation, they observed a higher ability of $+IF_1$ cells to alleviate such "ischemic" injury.

1.7.1 Reactive oxygen species in hypoxia

It has now been over 40 years since H_2O_2 generation from mitochondria was first recorded (72), quickly followed by the detection of mitochondrially generated superoxide anions ($O_2^{\cdot-}$) (73). These findings, together with the uncovering of superoxide dismutase (SOD) (74), an important antioxidant enzyme of the mitochondria matrix, prompted scientists to consider mitochondria as important sources of ROS in cells. The first ROS generated by mitochondria is $O_2^{\cdot-}$, as a result of monoelectric reduction of O_2. The continuous activity of the ETC principally reduces O_2 to water but a small amount of O_2 is reduced to $O_2^{\cdot-}$. Superoxide is mainly generated at complexes I and III (75) and released into the intermembrane space (approx. 80% of the generated superoxide) or the mitochondrial matrix (approx. 20%) (76). Being this species highly reactive, it is promptly converted into H_2O_2, thanks to the mitochondrial SOD (Mn-SOD or SOD2) and to the cytosolic SOD (CuZn-SOD or SOD1). Since the bulk of mitochondrial ROS generation is the ETC (77), this generation can occur at relatively high rates compared to cytosolic ROS production and is primarily determined by metabolic conditions. The result of generating ROS at potentially high rates and in a manner not primarily determined by signalling networks is that mitochondrially-generated ROS are associated mostly with damaging processes, although signalling roles for these species are now being uncovered, regarding cell function and homeostasis maintenance and signalling pathways regulation. As previously described, cancer cells experience a strong reduction of O_2 concentration and mitochondria are the main oxygen sensors in cells (over 90% of O_2 is used for mitochondrial respiration). In this scenario, the reactive oxygen species level in hypoxia is still unclear and needs to be addressed. Contrasting results are in fact reported: whereas some authors state that the decrease of O_2 as main substrate for ROS production leads to a decrease of ROS (78), others say that the minor availability of O_2 as final substrate of the ETC slows down the electron transport rate increasing electrons permanence time in the redox centres of the ETC, thus increasing ROS production (79) (80). The presence of ROS during hypoxia activates HIF-1α by inhibiting PHDs. This increases the activation of transcription factors not only involved in angiogenesis, erythropoiesis and glycolysis, but also in antioxidant defence, such as NRF2 (81). A further ROS increase causes DNA double strand breaks with increase in mutations (genomic instability) and cell damage (lipoperoxidation) leading to *necrosis* of cells that are more distant from vessels. However, the activation of HIF1-α by ROS in sublethally damaged tumor cells closer to the vessels, allows the expression of HIF1*α*-driven genes that contribute to their survival and growth thereby increasing their commitment to malignancy. It has also recently

been studied a relationship between the mitochondrial membrane potential and ROS levels (82): in HeLa cells, the addition of oligomycin-an important ATPase F_O-domain inhibitor- and the consequent $\Delta\psi_m$ increase, leads to a higher production of peroxides in mitochondria. Instead, the addition of FCCP is responsible for a sharp decrease of H_2O_2 amount. Considering the role played by IF_1 in the control of $\Delta\psi_m$ under stressing conditions, it could be interesting to analyse the differences in terms of ROS production in cells expressing different levels of IF_1.

In order to balance ROS production, cells are able to increase antioxidant systems expression and activity: the main endogenous antioxidants are represented by the glutathione system (GSH/GSSG and glutathione peroxidase -GPX), superoxide enzymes (SOD1 and SOD2), catalase, redoxins (thioredoxin, peroxiredoxin). Glutathione peroxidase is a family of potent antioxidant enzymes that are mainly responsible for scavenging excessive H_2O_2 and reducing lipid hydroperoxides. They catalyse the conversion of reduced glutathione (GSH) to GSSG in the presence of H_2O_2. GSH is then promptly regenerated by glutathione reductase (GR) in the presence of $NADPH^+$ and H^+ (83). Superoxide dismutases are important enzymes due to their crucial role in scavenging $O_2^{\cdot-}$. Specific metal atoms, such as copper (Cu), zinc (Zn), manganese (Mn), iron (Fe) and nickel (Ni), are essential cofactors of various types of SODs due to their high reactivity with $O_2^{\cdot-}$(84). They quickly convert $O_2^{\cdot-}$, highly reactive, into H_2O_2. Since the accumulation of H_2O_2 and its product, $OH^{\cdot}$ (hydroxyl radical) can cause severe oxidative damage to the cell, catalase, another important peroxides scanvenger, catalyses the conversion of peroxide into water (85) (86).

1.8 Importance of mitophagy in cellular balance

Autophagy is a degradative process by which cytosolic organelles and constituents are captured by phagophore membranes and degraded through fusion of the resulting autophagosomes with lysosomes. This mechanism is essential for the cell to get rid of non-functional or potentially toxic particles (87). In particular, mitophagy is the selective autophagic progress which targets mitochondria thanks to the interaction between adaptor molecules located in the OMM and processed LC3 (88). These adaptor molecules are BNIP3, NIX and FUNDC1 in addition to mitochondrial targets of E3 ubiquitin ligases, such as Parkin (PARK2) and PINK1. Mitophagy is responsible for the turnover of dysfunctional mitochondria that would otherwise damage the cell, and the main events preceding mitophagic pathway activation are loss of $\Delta\psi_m$ and mitochondria fragmentation. Mitochondrial membrane depolarization also induces proteolytic

cleavage and degradation of the fusion protein Opa-1 thereby reducing the size of mitochondria, a consequence favouring the uptake of mitochondria by phagosomes (89). On the other hand, mitochondrial fusion protects healthy respiring mitochondria from degradation, a mechanism that is promoted by protein kinase A (PKA)-mediated inhibition of the fission protein Drp-1.

The accumulation of non-functional mitochondria is often associated to aging process probably due to an increase of free radicals production. However, mitophagy also plays a key role in reducing mitochondrial mass in the acute response to certain stresses, such as hypoxia and nutrient deprivation (90) occurring in cancer. It has been observed in HeLa cells that when $\Delta\psi_m$ is compromised, the dimerization of IF_1 and its binding to the ATP synthase promotes PINK1 stabilization on the OMM (91). This is a critical step in recruiting PARK2 and activating mitophagy.

1.9 Mitochondrial contribution to apoptosis

The beginning of apoptosis (programmed cell death) is regulated by the activation of caspases, a group of cysteine proteases normally existing as pro-caspases. During apoptosis, they are cleaved to generate active caspases, the enzymes responsible for the cleavage of many cellular substrates to dismantle cell content (92). Two main apoptotic pathways are known: extrinsic and intrinsic pathways responding to different signals. The extrinsic signalling pathways that initiate apoptosis are characterized by transmembrane receptor-mediated interactions, involving death receptors that are members of the tumor necrosis factor (TNF) receptor gene superfamily (93). TNFs play a critical role in transmitting the death signal from the cell surface to the intracellular signalling pathways. The best-characterized ligands and corresponding death receptors include FasL/FasR, TNF-α/TNFR1, Apo3L/DR3, Apo2L/DR4 and Apo2L/DR5. Following ligand binding, cytosolic adapter proteins are recruited to regulate the downstream activation of caspase-8. Once caspase-8 is activated, apoptosis is triggered. The intrinsic pathway is also known as mitochondrial pathway considering the essential involvement of mitochondria in this process. These organelles are in fact essential for the handling not only of anti-apoptotic and pro-apoptotic proteins interactions, but also for the regulation of signals that initiate the caspases activation. Cytocrome c is a key component of the apoptotic event, since its release from the IMM triggers the activation of caspase 9. Activated Caspase-9 further cleaves downstream caspases such as Caspase-3, -6 or -7 (94). The permeability of the IMM needs indeed to be strictly regulated: important regulators of cyt c release are Bcl2 proteins,

that, together with other many anti-apoptotic regulators, such as Mcl-1 and A1, are able to counteract the activity of pro-apoptotic factors (Bax, Bak, Bok) (95). Another important aspect involved in the IMM permeability is the opening of the multiprotein pore PTP located in the contact site between the outer membrane and inner membrane (96). Opening of PTP leads to matrix swelling, depolarization of the inner membrane (dissipation of the $\Delta\psi_m$), ensuing rupture of the outer membrane, and nonselective release of IMS proteins. All these events represent the unavoidable prelude to programmed cell death.

However, the link between apoptosis and cancer emerged when Bcl2 proteins family was discovered (97). This gave birth to the concept that compromised apoptosis is a central step in tumorigenesis. Indeed, a defective suicide programme endows nascent neoplastic cells with multiple selective advantages: cells can survive in hostile places where, for instance, nutrients or oxygen are limiting, evolving into more aggressive derivatives. Thus, cells become more resistant and able to survive detachment from the extracellular matrix and to migrate (metastasis).

1.10 Mitochondrial Ca^{2+} homeostasis regulation

Cells invest much of their energy to control cytosolic Calcium (Ca^{2+}) concentration, which needs to be maintained ~100 nM. Many ways to sequester Ca^{2+} from the cytosol have been developed, favouring its binding energy for signal transductions. To exert control over Ca^{2+}, cells must extrude it, chelate it, or compartmentalize it. The main protagonists of Ca^{2+} extrusion from cytosol to extracellular space are Na^+/Ca^{2+} exchangers (NCX), Na^+/Ca^{2+}, K^+ exchangers (NCKX), Ca^{2+} -activated Cl^- and K^+ channels, plasma-membrane Ca^{2+} receptors (PMCA), Voltage-gated Ca^{2+} selective channels (CaVs). Ca^{2+} is indeed chelated in the cellular environment by EDTA and EGTA and is stored in specific Ca^{2+} compartments represented by endoplasmic reticulum (ER) and mitochondria [Fig.12]. Hundreds of proteins have been adapted to bind Ca^{2+} in order to buffer its level or trigger signalling pathways. Among these, calmodulin is the most important protein involved in Ca^{2+} signalling. It is a small ubiquitously expressed adaptor protein that changes its domains shape upon Ca^{2+} binding. Under such circumstances, hydrophobic surfaces are exposed within each domain of the protein, triggering calmodulin Ca^{2+} sensor activity (binding to its targets). Hydrophobic residues, usually containing methionine, wrap around amphipathic regions of target proteins, such as the α-helices in myosin light chain kinase (MLCK) and calmodulin dependent kinase II (CaMKII).

Calmodulin also extends the reach of Ca^{2+} by activating phosphorylation pathways. Ca^{2+}/calmodulin binding relieves autoinhibition of the catalytic domain of calmodulin kinase (CaMK) family enzymes. CaMKIIs multimerize, leading to interphosphorylations that prolong kinase activity (98).

Increases in cytosolic Ca^{2+} concentration are mainly associated to its release from the external medium or from intracellular stores. In the first case, the different plasma-membrane channels are activated in response to stimuli including membrane depolarization, toxic stimuli, extracellular agonists and intracellular messengers. In the second case, Ca^{2+} is normally released from the endoplasmic reticulum, ER (or its equivalent in myocytes, the sarcoplasmic reticulum - SR) following stimuli coming from Ca^{2+} itself or other messengers, such as inositol-1,4,5-trisphosphate ($Ins(1,4,5)P_3$), cyclic ADP ribose (cADPR), nicotinic acid adenine dinucleotide phosphate (NAADP) and sphingosine-1-phosphate (S1P) (99).

Inositol triphosphate (IP_3) pathway relies on the previous activation of phospholipase C (PLC). There are several PLC isoforms, activated by different mechanisms, e.g. G-proteins and tyrosine-kinase coupled receptors, increases in Ca^{2+} concentration, Ras activation (100). Once activated, PLCs hydrolyse phosphatidylinositol 4,5 bisphosphate (PIP_2), a phospholipid located in plasma membrane, to diacylglycerol (DAG) and IP_3. IP_3 works as messenger for the mobilization of Ca^{2+} from ER by activating IP_3 receptors (IP_3R) placed on the ER-membrane (or ryanodine receptors -RyR- in case of myocytes). The release of Ca^{2+} from ER via IP_3 pathway can be driven by either endogenous stimuli or exogenous molecules, such as Histamine in HeLa cells (101) (102). Ca^{2+} release from ER is rapidly counteracted by SERCAs pumps (sarco-endoplasmic reticulum Ca^{2+} ATPases) situated on the ER membrane, that try to maintain physiological Ca^{2+} levels driving this ion back to ER by using ATP. Upon pharmacological stimulus with Histamine, HeLa cells show in fact oscillations of cytosolic Ca^{2+} concentration due to alternated releases and uptakes (102). Once Ca^{2+} is released, it is promptly accumulated in cytosol and in mitochondria, given the close proximity of the latter to ER (103).

Mitochondria are therefore one of the main targets, and at the same time regulators, of Ca^{2+} signalling, since their function, movement and viability are tightly associated to this ion. Like the ER, mitochondria can also store mM concentrations of Ca^{2+} but in mitochondria it is regulated by fundamentally distinct mechanisms compared to those used in the ER. Whereas Ca^{2+} readily diffuses through large pores in the mitochondrial outer membrane, it crosses the inner membrane via ion channels and transporters. Outer membrane's TSPO (104) and VDAC

(105) take part to the mitochondrial uptake of Ca^{2+} and other ions. In particular, although originally thought to be exclusive component of the OMM, it has been then demonstrated that VDAC is located in the contact sites between the OMM and the ER, consequently increasing its participation to mitochondria/ER Ca^{2+} signalling. As introduced, the mechanisms involved in Ca^{2+} transport through the IMM are more complex: accordingly, a rapid electrogenic pathway, denoted the "mitochondrial calcium uniporter" (MCU), quickly transports Ca^{2+} into the matrix, driven by the negative charge of the membrane potential established by the respiratory chain (106). MCU-mediated Ca^{2+} uptake is partly inhibited at basal and low concentrations of cytosolic Ca^{2+} by the regulator MICU1(107) (108). Signalling by G protein-coupled receptors or tyrosine kinases receptors, that increase cytosolic Ca^{2+} concentration above 3 μM, stimulates MCU current (I_{MCU}), resulting in the accumulation of Ca^{2+} in the mitochondrial matrix. Changes in cytosolic Ca^{2+} content activate numerous transcription factors, such as nuclear factor of activated T cells (NFAT), c-FOS, and cyclic AMP response element binding protein (CREB). The latter is activated by phosphorylation when cytosolic Ca^{2+} concentration increases, due to IP_3R-mediated release or plasma membrane SOCE (store-operated Ca^{2+} entry), resulting in the activation of genes involved in Ca^{2+} buffering: it has been demonstrated that in HeLa cells CREB binds MCU promoter actively stimulating MCU abundance in the cell (109). Mitochondria that have accumulated Ca^{2+} exhibit higher mitochondrial bioenergetics through tricarboxylic acid (TCA) cycle and oxidative phosphorylation (110). In general, increases in the concentration of Ca^{2+} ions in the cytoplasm are important for the initiation of cellular processes such as contraction, secretion, ion- and metabolite- pumping and proliferation. These processes are energy requiring and are associated with an increased need of ATP, which has to be matched with an increase in ATP supply. The increased ATP synthesis is reached by activating the intramitochondrial Ca^{2+}-sensitive dehydrogenases and hence through increases in NADH supplied respiration (110). In particular, it was observed that Ca^{2+} interacts with the following mitochondrial enzymes: FAD-glycerol phosphate dehydrogenase (FAD-GPDH); pyruvate dehydrogenase phosphatase (PDHP), involved in the induction of the rate-limiting step for mitochondrial respiration activation through Acetyl-CoA production (111); NAD^+-isocitrate dehydrogenase (NAD-ICDH) and 2-oxoglutarate dehydrogenase (OGDH), both involved in Kreb's cycle; ATP synthase. Although shown to bind Ca^{2+} directly through F_1 β-subunit (112), the ATP synthase is likely to be regulated via post-translational modifications, such as phosphorylation of the γ-subunit which was found to be sensitive to mitochondrial Ca^{2+}. Recent work has identified a protein that binds to ATP synthase in Ca^{2+}-dependent manner in cardiomyocytes, resulting in an increased

capacity for ATP production (113). At the present time, other potential mitochondrial targets for Ca^{2+} are being studied, like cytocrome c oxidase, malate-aspartate shuttle, pyrophosphatase, ATP-Mg2+/Pi transporter (114). Increasing ATP production means that more oxygen is reduced to water, but at the same time a higher number of electrons can escape from ETC's complexes giving the formation of superoxides that could damage mtDNA. For this reason, mitochondrial Ca^{2+} concentration must be controlled, in order to avoid the final activation of apoptotic pathways. Ca^{2+} overload in mitochondria is also associated to mitochondrial swelling, which could lead to IMM impairment and eventually outer membrane rupture and release of apoptotic proteins (115).

Given the role of IF_1 in regulating ATP synthase activity and $\Delta\psi_m$, essential for Ca^{2+} entry in mitochondria, a possible involvement of the protein in mitochondrial Ca^{2+} signalling will be addressed.

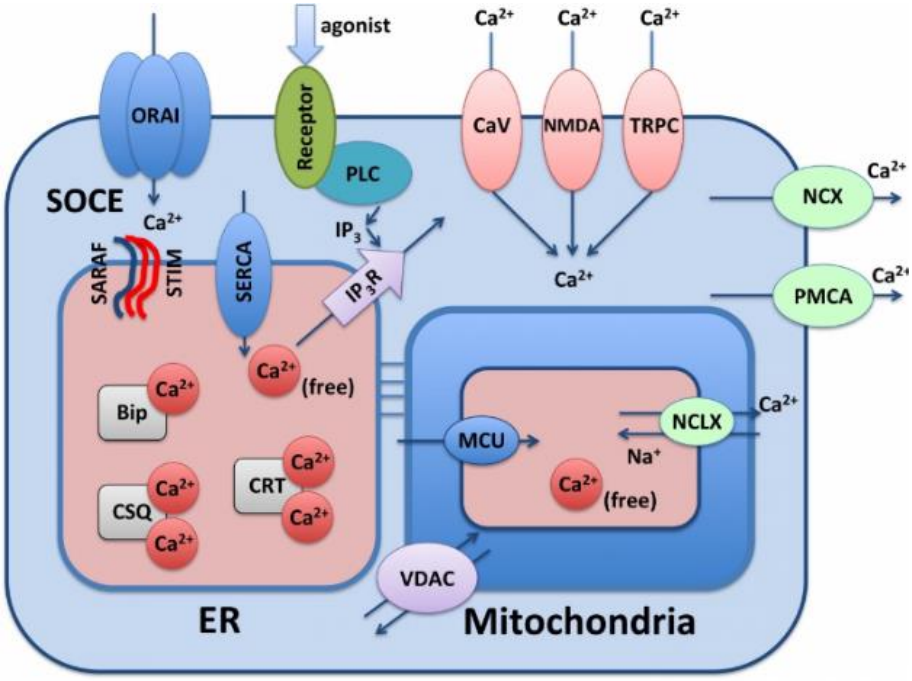

Fig. 12. Ca^{2+} signalling and crosstalk between ER and mitochondria [Reuveny E., Weizmann Institute of Science]

1.11 Highlights on the cell lines used

1.11.1 HeLa cell line

Cervical adenocarcinoma is an epithelial tumor of the cervix uteri with a high level of mortality in developing countries. Human papillomavirus (HPV) has been identified as one of the prime etiologic agents in the progress of the cervical neoplasia. For this reason, screening programs are normally run in women of fertile age. HPVs are specific and tissue trofic, and able to grow and survive in completely differentiated epithelial cells. There are more than 100 HPV genotypes, categorised in high and low risk groups. HPV-16 and HPV-18 are considered the high risk types and responsible for malignancy development. Besides the oncogenic potential of HPV infection, many other risk factors concur in the etiology of this disease, such as nutrients deficiency, low socioeconomic status, high usage of oral contraceptives, genetic factors (116). At the present time, chemoradiotherapy and surgical removal are the most used medical approaches towards the disease (117).

HeLa cells (human cervical adenocarcinoma cells) [Fig. 13] are one of the most important tumor cell lines in the field of scientific investigation. They are known as the first immortal cell line ever used in research laboratories and their story is quite extraordinary: the acronym "HeLa" means "Henrietta Lacks", which is the name of a 31 years old African American woman who was diagnosed with cervical adenocarcinoma in 1950s during her hospitalization at the Johns Hopkins Hospital in Baltimore, Maryland (118). Henrietta's cells were taken without her knowledge by researcher George Gey, who started to use and expand them to carry out his experiments. After her death, a huge debate rose up, especially because Henrietta never had the chance to know what had happened with her cervical cells and, moreover, her unaware donation hadn't been anonymous. In those years there wasn't any attention to ethical problems in the field of scientific research, although getting human samples for research purposes without consent is illegal nowadays.

However, HeLa cells represented a great step forward in science, since until 1950s all the cells available for the experimentation died after a few replications. Scientists soon realized that for the first time in history they would use an *immortal* cell line, which means that cells had the incredible ability to divide indefinitely, giving birth to a great opportunity for cancer research progress. From that moment on, HeLa cells have represented an important cellular model for

cancer biology, gene mapping, gene transfection techniques, pharmacology and toxicology studies, just consider that the first achievement reached was the development of the polio vaccine in 1953 (119).

As previously introduced, mitochondrial ATPase inhibitory factor 1 (IF_1) was found to be up-regulated in many human carcinomas (51). Accordingly to these evidences, human cervical adenocarcinoma cells have been chosen to study IF_1 involvement in cellular Ca^{2+} homeostasis regulation.

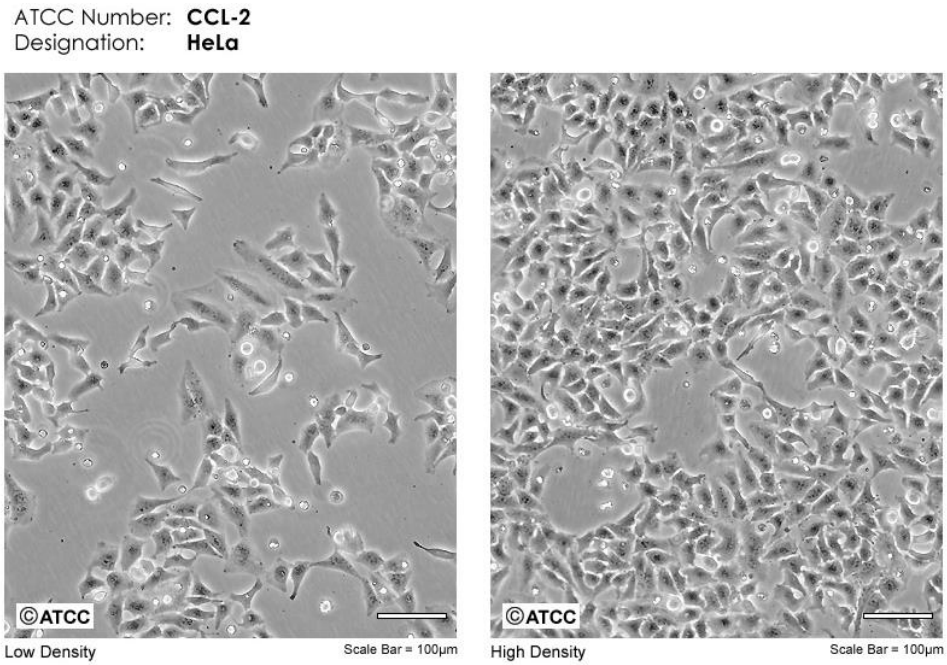

Fig. 13. Optical microscope images of HeLa cell line [ATCC registered trademark]]

1.11.2 143B cell line

Osteosarcoma is an uncommon cancer which arises from bone. Despite its very low incidence, osteosarcoma predominantly affects adolescents and young adults. Modern therapy is represented by chemotherapy, radiotherapy and surgery but still, the survival rate of patients diagnosed with the disease is not high, due to the high propensity of this malignancy to metastatization, especially in lungs (120). Hence, the interest towards novel approaches or optimization of the current strategies for treating the disease has grown consistently. Anatomically, osteosarcoma shapes in the metaphyseal region of long bones, within the medullary cavity, and infiltrates into the bone also involving the surrounding tissues (121).

Histologically, it is characterized by fusiform cells producing an osteoid matrix. It was first suggested that the main reason that could promote osteosarcoma's onset was the interaction with the external environment, in particular radiations or chemical agents. Later on, the improvement of the molecular techniques has allowed to identify several chromosome abnormalities and genetic syndromes (i.e. Fraumeni syndrome, retinoblastoma) that could be associated with this neoplasia (122). In fact, it has been demonstrated that alterations in oncosuppressor genes can directly participate to osteosarcoma pathogenesis: for instance, p53 gene is mutated in the 22% of all osteosarcomas and mutations in oncosuppressor Rb influence osteosarcoma's carcinogenesis by impairing cell cycle (123). Increased cell proliferation rate and metastatization have also been related to mutations in AP-1 (involved in cell proliferation and differentiation mechanisms and bone metabolism control), myc up-regulation (probably associated with an increased resistance towards chemotherapy), augmented growth factors activation and receptors overexpression (TGF, IGF, CTGF) (124) (125). In addition, the stabilization of the hypoxia inducible factor 1 (HIF-1) and the consequent activation of the proangiogenic VEGF have been observed in the cells located in the central areas of the tumor (126).

Considering all these aspects, a great interest towards both clinical and molecular mechanisms behind osteosarcoma pathogenesis has recently developed.

An initial screening performed in our laboratory showed that mitochondrial ATPase inhibitory factor 1 (IF_1) is up-regulated in osteosarcoma cell line. Hence, 143B cells have been chosen to stably silence the expression of the protein and investigate its role in bioenergetics regulation under both physiological and stressing/hypoxic conditions.

2 AIM OF THE STUDY

Tumor cells metabolism has been widely investigated and nowadays it is one of the major topics researchers are focused on, with the final purpose to find therapeutic strategies to inhibit cancer growth and metastasis. Nevertheless, before setting up therapeutic approaches, it is fundamental to deeply investigate and understand the basic mechanisms occurring in malignant transformation. One of the first aspects that was discovered is the metabolic switch towards aerobic glycolysis (5) to sustain the enhanced energy demand necessary for cancer cells growth and proliferation. This mechanism, known as *Warburg's effect*, has been then challenged by many studies which demonstrated an important contribution of mitochondria to tumor cells metabolism. For instance, 143B (osteosarcoma) and HeLa (cervix adenocarcinoma) cell lines, used in the present study, rely on oxidative phosphorylation as major source for energy production (64) (65).

An important feature of solid tumors is the high vascularization degree, created by both pre-existing and new-generated blood vessels, to ensure the sufficient nutrients intake. However, blood vessels often undergo damage and impairment and the cells localised in the most central areas of the tumor end up being far from the capillary endothelium, experiencing conditions of severe hypoxia/anoxia (67).

Taking all these aspects into account, the role of mitochondrial F_1F_O-ATPase Inhibitory Factor 1 (IF_1) will be addressed. IF_1 is an endogenous, ubiquitously expressed, nuclear encoded protein of ~10 kDa, highly conserved among species. It was first discovered by Pullman and Monroy in 1963 (42) and described as inhibitor of the hydrolytic activity of the mitochondrial ATP synthase. Under normoxic physiological conditions, the mitochondrial ATP synthase uses the proton electrochemical gradient created by the mitochondrial electron transport chain (ETC) to synthesise the most powerful source of energy in the cell, the ATP molecule. Under certain circumstances, such as hypoxia/ischemia, the proton electrochemical gradient may be lost, due to a dramatic impairment of the electron transport across the enzyme complexes of the ETC, allowing the ATP synthase to reverse its activity and hydrolyse cytosolic ATP to restore the proton gradient essential for cell survival. This ATP consumption needs to be strictly regulated in order to avoid a complete energy depletion. The acidification of the mitochondrial matrix caused by the collapse of the inner membrane potential ($\Delta\psi_m$) induces the activation of IF_1 by disrupting the tetrameric form of the protein and generating active dimers (43). The active forms

of the inhibitor bind the αβ interface of ATP synthase's F_1 portion and block its hydrolytic activity.

Besides the canonical role in protecting tumor cells from ATP wasting, many other aspects concerning IF_1 presence in tumors need to be considered: for instance, it is overexpressed in many human carcinomas (52) where it may promote cancer cell growth and proliferation. In addition, it may be involved in ATP synthase oligomerization modulating apoptosis and autophagy processes (58). Moreover, its involvement in cancer cells metabolism regulation under physiological conditions has been scarcely addressed: for this reason, the first part of this dissertation will be focused on the investigation of the function exerted by IF_1 in human cancer cells bioenergetics under normoxic conditions (21% O_2). Considering the importance of $\Delta\psi_m$ in the regulation of many cellular functions, i.e. molecules transport, apoptosis regulation, ROS production and ions homeostasis control, we will first try to shed light on the possible involvement of IF_1 in mitochondrial Ca^{2+} handling. Mitochondria are important Ca^{2+} storage sites in cells, together with the endoplasmic reticulum (ER) and a functional cross talk between the two organelles occurs to monitor cytosolic Ca^{2+} concentration, given the close proximity of the two cellular compartments (103). Both cytosolic and mitochondrial free Ca^{2+} levels will be analysed in IF_1 expressing and non-expressing HeLa cells and related to mitochondrial Ca^{2+} uniporter (MCU) expression levels and $\Delta\psi_m$, previously addressed (56). Mitochondrial $\Delta\psi_m$ analysis in normoxia will be then deepened in 143B osteosarcoma cell line, stably silenced for the inhibitor protein. The data obtained will be then related to the study of the oligomeric organization of the ATP synthase in the presence or absence of the protein, in order to finally clarify this matter. In fact, contrasting data are reported in literature: while some investigators observe that IF_1 may directly contribute to the dimerization of the enzyme (49) (58), others say that the arrangement in oligomers might be independent from IF_1 binding (57) (59).

Once clarified the involvement of IF_1 in tumor cells bioenergetics modulation in normoxia, a new set of data will be discussed regarding tumor cells inner membrane function alterations under stressing/ischemic conditions, by using an Invivo2 hypoxic chamber to mimic the typical hypoxic environment found in central areas of solid tumors (0.5% O_2).

For these purposes, stably IF_1-silenced 143B and HeLa cells will be used and compared with parental and scrambled cells to understand the role played by IF_1 in cancer metabolism. A complete elucidation of this topic could be interesting for the creation of new therapeutic strategies targeted to the inhibition of tumor cells growth and proliferation.

3 MATERIALS AND METHODS

3.1 Cell Cultures and transfections

Human osteosarcoma 143B cells were grown and maintained in Dulbecco's Modified Eagle Medium (DMEM) supplemented with 10% bovine serum, 100 U/ml penicillin, and 100 µg/ml streptomycin 0.25 µg/ml amphotericin B, 4 mM glutamine, 25 mM glucose and 1 mM pyruvate at 37°C in a humidified atmosphere (5% CO_2). For transient cotransfection we used pCMV6-XL5-IF1 expression plasmid together with alternatively a single shRNA vector or a scrambled negative control construct cloned in a pGFP-V-RS plasmid (#1 GI325933, #2 GI325934, #3 GI325935, #4 GI325936 and TR30013, respectively). All the plasmids used were from Origene (Rockville, MD, USA). Equal amounts of the two vectors (4 µg total DNA) were transfected overnight using polyethylenimmine (PEI). After 24 h the medium was replaced with complete DMEM and the cells were cultured for further 24 hours before analysing IF_1 silencing level. To establish stable clones, parental 143B cells were seeded and transfected as described above with 2 µg of either GI325936 or TR30013 plasmid DNA. Cells were split and selected for stable transformation 48 hours later, in the presence of 1 µg/ml puromycin, and the culture medium was changed every day. Single colonies were then subcloned by limiting dilution and finally all the clones obtained were assayed for IF_1 expression by Western Blotting technique.

Once confirmed the stable silencing of IF_1, the cells were used for all the experiments according to the following procedure: after being seeded on the first day, the medium was replaced on the second day with a new and fresh complete DMEM and the cells were moved either to the incubator (for the normoxic exposure) or to a Invivo2 hypoxia chamber (Ruskinn technologies) for 24 or 48 hrs.

During my stay in London, HeLa (cervix adenocarcinoma) cells were used for the experiments regarding mitochondrial Ca^{2+} signalling in live-imaging. Cells were previously transfected with a silencing RNA (siRNA) which targets the mRNA of IF1 (QIAGEN S100908075) and with a scrambled plasmid as control, according to the method described in Campanella et al, 2008 (49) and stable IF_1-silenced clones were obtained, confirmed by Western Blotting technique. In order to carry out the study, cells were grown in complete DMEM (Life Technologies, Inc.) supplemented with 10% FBS, 100 units/ml penicillin, and 25 mg/ml streptomycin. They were kept in T-75 (250 ml) Falcon flasks, and incubated at 37°C in a 5% CO_2 humidified incubator.

Once they reached 50%–60% confluence, cells were split and cultured on round borosilicate cover glasses (VWR, Radnor, PA, USA), and mounted within an Attofluor® metal cell chamber for microscopy (Molecular ProbesTM, Thermo Fisher Scientific, A-7816) prior to experiment.

In order to fully clarify the involvement of IF_1 in mitochondrial Ca^{2+} handling transient transfection were performed to induce either increased IF_1 expression or mutation in IF_1 active sequence. Up-regulation of the protein was achieved by using the full-length ORF cDNA clone of human ATPase inhibitory factor 1 (ATPIF1), transcript variant 1, mRNA (321 bp; GenBank® accession number: NM_016311.4). The 19 fluorescent-tagged version of IF_1, obtained by fusion with EYFP, was obtained by subcloning of the protein cDNA, excised from pCMV-Sport6-ATPIF1, into the MCS of the plasmidial vector pEYFP-N1. The procedure was carried out by Mutagenex (Suwanee, Georgia, United States). IF_1 mutant H49P clone was obtained by Site-directed mutagenesis and subcloning of the mutated cDNAs into pEYFP-N1 which was realized by Mutagenex.

Cells were seeded on glass coverslips for microscopy on the first day and transfected on the following day by using Lipofectamine p3000 vector (Thermo Fischer Scientific) according to the manufacturer instructions. After 24 h cells were washed in PBS (Life Technologies, Inc.) and left for further 24-36 h prior to experiment.

3.2 Cell Growth

Cell growth was assessed after seeding 2×10^5 cells in complete DMEM and culturing the cells for up to 72h. Adherent cells were trypsinized and collected, and the growth of cell lines was assayed using the trypan blue exclusion test. Cell count was performed every 24 h without changing the medium.

3.3 Mitochondrial Isolation

Coupled mitochondria were isolated from cells according to the method described by Barbato S. et al. (57). After collecting the cells from the Petri dishes and washing them in Hank's balanced salt solution - HBSS (0.4 g/L KCl, 0.06 g/L KH_2PO_4, 0.35 g/L $NaHCO_3$, 8 g/L NaCl, 0.05 g/L Na_2HPO_4, pH 7.4), cells were homogenized by using a glass Potter-Helvehjem homogenizer with a motor-driven Teflon pestle in isolation buffer (0.22 M mannitol, 0.07 M

sucrose, 0.02 M HEPES, 1 mM K-EDTA, 0.1 mM K-EGTA, pH 7.4) containing 1 mM PMSF (phenylmethanesulfonyl fluoride). Crude extracts were centrifuged at 2000 rpm for 10 min (Sorvall SS34 rotor) to remove nuclei and plasma membrane fragments, and then the supernatant was centrifuged at 10000 rpm for 10 min (Sorvall SS34 rotor) to obtain the mitochondrial fraction. Mitochondria were washed in 0.25 M sucrose, 0.02 M HEPES, 1 mM KEDTA and 0.1 mM K-EGTA, pH 7.4 and suspended in the same buffer at 10 mg/ml of protein concentration verified by Lowry quantification assay.

3.4 BN-PAGE Analysis and Western Blot

The organization of the ATP synthase complex and the binding of IF_1 to the monomeric and/or oligomeric form of the enzyme were analyzed by 1D blue-native PAGE (6). Mitochondria were treated with digitonin in a ratio of 2.5:1 (w/w) digitonin/mitochondrial protein. Once permeabilized, the mitochondrial extracts were treated with Coomassie Blue dye and loaded into a native gel (3.5%-7% acrylamide/bis-acrylamide). Following overnight electrophoresis in non- denaturating conditions, proteins were immediately electroblotted onto nitrocellulose membranes in denaturing conditions. Right afterwards, ATP synthase and IF_1 protein bands were detected using anti-α and anti-d subunits and anti-IF_1 primary monoclonal antibodies (MitoSciences Inc., Eugene, OR, USA), respectively, and a secondary goat anti-mouse IgGH+L antibody labelled with horseradish peroxidase (Life Technologies, Carlsbad, CA, USA). The immunoblots were detected and quantified by chemiluminescence using the ECL Western Blotting Detection Reagent Kit (Amersham Biosciences, Piscataway, NJ, USA).

3.5 In-gel ATPase Activity

Right after the electrophoretic run of the protein complexes extracted from digitonin-treated mitochondria, ATPase activity was assayed on the native gel by using an enzymatic colorimetric method based on the formation of a white lead phosphate precipitate formed by the ATP hydrolysis activity (127). White-stained ATP synthase bands were acquired using a GS-800 densitometer (BioRad, Hercules, CA, USA) with a blue filter to minimize the interference from the residual Coomassie Blue.

3.6 SDS-PAGE and Western Blot

Cells were collected from the Petri dishes and washed in Hank's buffer, and immediately treated with RIPA lysis buffer (50 mM Tris HCl, 150 mM NaCl, 0.5% sodium deoxycolate, 1% SDS, pH 8) at 4°C, supplemented with protease inhibitors cocktail and 1mM of PMSF in order to prevent proteins degradation. Following the quantification by Lowry assay, the protein lysates were then supplemented with Laemmli-sample loading buffer (0.102 g/ml SDS, 0.36 ml/ml Glycerol, 0.357 ml/ml TRIS HCl pH 6.8, 0.5 µl/ml β-mercaptoethanol, 0.7 mg/ml bromophenol blue) and loaded into a SDS polyacrylamide gel. Cellular lysates were separated by SDS-PAGE and blotted onto nitrocellulose membranes to perform semiquantitative analysis of protein content according to Baracca et al. (128). Blots of resolved proteins were incubated with primary mouse monoclonal antibodies specific for the d-subunit (19 kDa) and the β-subunit of F_1F_0-ATPase (52 kDa), IF_1 (12 kDa), and with primary rabbit polyclonal antibodies specific for MCU (50 kDa). A cocktail of five primary mouse monoclonal antibodies specific for single subunits of each OXPHOS complex (MitoSciences Inc., Eugene, OR, USA) was used as reported in Sgarbi et al. (129),. Actin (42 kDa) and porin (35 kDa), used as loading controls for cells and mitochondria respectively, were immunodetected with mouse monoclonal anti-actin (Sigma-Aldrich, St. Louis, MO, USA) and anti-porin (Mito-Sciences Inc., Eugene, OR, USA) primary antibodies. Immunodetection of primary antibody was carried out with secondary goat anti-mouse IgGH+L antibody (Life Technologies, Carlsbad, CA, USA) labelled with horseradish peroxidase. Chemiluminescent detection of the specific proteins was performed with the ECL Western Blotting Detection Reagent Kit (GE Healthcare, Waukesha, WI, USA), composed by peroxide (H_2O_2) and luminol: peroxide is quickly hydrolized by the peroxidase enzyme bound to the secondary antibody into H_2O and O_2. The O_2 produced is directly involved in luminol oxidation and in light production. The emitted luminescence was detected by using the ChemiDoc MP system equipped with the ImageLab software (BioRad, Hercules, CA, USA) essential to perform the densitometric scanning of the relative protein intensity.

3.7 Flow Cytometric Assessment

Fluorescence level of GFP positive cells was analysed by flow cytometry using a FACSaria cytometer (Becton Dickinson, Franklin Lakes, NJ, USA). Excitation was at 488 nm and fluorescence emission was measured at 530/30 nm. Data acquisition and analysis was performed with BD FACSDiva and Flowing Software, respectively.

3.7.1 Mitochondrial membrane potential measurement

The inner mitochondrial membrane potential ($\Delta\psi_m$) was measured by staining cells with 20 nM tetramethylrhodamine methyl ester (TMRM, Molecular Probes, Eugene, OR, USA), a lipophilic cationic probe which passes through biological membranes and enters mitochondria in a $\Delta\psi_m$-dependent manner (130). Cells were incubated with the probe for 30 min at 37°C in the presence or absence of 0.6 μM oligomycin and were then washed twice with Hank's buffer to remove any remaining unincorporated dye. Cells were rapidly trypsinized, diluted to the optimal density (300.000 cells/ml) with Hank's buffer and supplemented with 10% FBS and analysed with the MUSE Cell analyser (Millipore, Billerica, MA, USA). Excitation was at 532 nm and fluorescence emission was measured at 576/28 nm. Data acquisition and analysis was performed with MuseSoft Analysis and Flowing software, respectively.

3.8 Brightfield and Fluorescence Microscopy

Brightfield and fluorescence images of controls and IF_1 silenced cells were acquired using a fluorescence inverted microscope (Olympus IX50 equipped with a CCD camera). Multiple high-power (magnification 10x and 40x) images were acquired with IAS2000 software (Delta Sistemi, Roma, Italy). Fluorescence photographs of GFP positive cells were obtained using a specific set of filters: excitation 480/30 and emission 530/30. Mitochondrial network morphology and membrane potential were evaluated by incubating cells with 20 nM TMRM for 30 min. At least 10 different optic fields were acquired for every experimental condition.

3.9 Biochemical Assays

3.9.1 Glucose consumption and lactate release measurements

Cells media were collected from the Petri dishes and immediately used for the glucose consumption and lactate release assays. These biochemical measurements were performed by using the Glucose Liquid Trinder Method Kit (FAR, Verona, Italy) and Lactate PAP Fluid Kit (Centronic GmbH, Wartenberg, Germany), respectively, following the manufacturer's instructions.

Glucose quantification was obtained by applying the colorimetric Trinder GOD/POD Method, universally used for the estimation of glucose in serum and plasma. The enzymatic reaction sequence employed in the assay of glucose is the following:

$$\beta\text{-D-Glucose} + H_2O + O_2 \xrightarrow{\text{Glucose oxidase}} H_2O_2 + \text{D-Gluconic Acid Peroxidase}$$

$$H_2O_2 + \text{4-Aminoantipyrine} + \text{Phenol} \xrightarrow{\text{Peroxidase}} \text{Iminoquinone (}\mathbf{\text{coloured compound}}\text{)} + H_2O$$

The increase in the absorption at 510 nm is proportional to glucose concentration and can be measured with the spectrophotometer.

Lactate quantification was performed by employing a colorimetric assay for the determination of lactate concentration in serum and plasma, as following:

$$\text{L-Lactate} + O_2 \xrightarrow{\text{Lactate oxidase}} \text{Pyruvate} + H_2O_2$$

$$H_2O_2 + \text{p-Aminophenazone} + \text{p-Clorophenol} \xrightarrow{\text{Peroxidase}} \text{chromogen} + H_2O$$

The increase in the absorption at 546 nm is proportional to lactate concentration and can be measured photometrically.

Data were expressed as µmol/10^6 cells and normalized to the number of cells present in the wells.

3.9.2 ATP levels measurement

The ATP content of cells was assayed by using a bioluminescence method based on the luciferin– luciferase system (ATP bioluminescent assay kit CLS II; Roche, Basel, Switzerland). Cells were trypsinized and washed in buffer containing 10mM Tris HCl, 100 mM KCl, 5 mM KH_2PO_4, 3 mM EGTA, 2 mM $MgCl_2$ pH 7.4. They were then suspended in the same buffer and a small amount of suspended cells was diluted in dimethyl sulphoxide (DMSO) to extract the intracellular content. The DMSO diluted cells were immediately cooled down with cold water

and placed on ice to stop ATP degradation. ATP content measurement was then performed adding the cellular extract to 0.1 M Tris/acetate, 2 mM EDTA pH 7.75 buffer and stocked luciferin, and referred to 1.65 mM standard ATP. The luminometric reaction induced is the following:

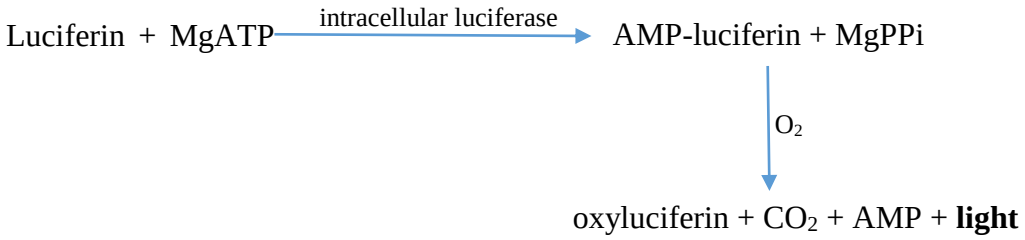

The amount of ATP measured is proportional to the amount of light emitted by the samples and recorded by the luminometer machine. It was referred to the protein content, determined by the Lowry method (explained below), and expressed as nmol of ATP/mg protein.

3.9.3 Citrate synthase activity assay

Citrate synthase (CS) is located in mitochondrial matrix and it is responsible for the first reaction of the Krebs cycle. For this reason, it is considered an important index of mitochondrial mass in the cells. The reaction catalysed by the enzyme is the following:

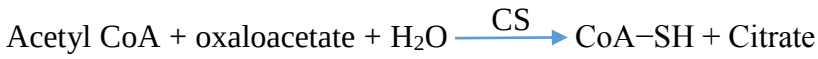

Reduced CoA reduces in turn 5,5’ dithiobis - 2’nitro-benzoic acid (DTNB) to TNB which is coloured, and the developed colour is recorded in a V-450 Jasco spectrophotometer. The overall reaction product, TNB, absorbs at 412 nm.

In order to perform this assay, cells were trypsinized and washed in Hank’s buffer and then suspended in the same. A small aliquot of cells was added to 125mM Tris HCl pH 8 buffer, Triton detergent (Sigma-Aldrich) to allow the permeabilization, DTNB, Acetyl CoA and oxaloacetate. Increased TNB production and absorption over time were observed in the graph. The assay was carried out at 30°C temperature and 412 nm wavelength. The specific activity

of the enzyme was calculated through Lambert-Beer Law application and it was referred to protein amount determined by the Lowry method and expressed as nmol/min/mg of protein.

3.9.4 Oxygen consumption rate measurement

The oxygen consumption rate was measured using an oxygen Clark-type electrode as reported by Baracca et al. (128). It is composed of a Pt cathode and an Ag/AgCl anode immersed in a KCl electrolytic solution and it's separated from the sample's suspension thanks to a gas semi-permeable membrane through which O_2 diffuses. The electric current generated by the redox reaction is proportional to the amount of O_2 that diffuses through the membrane and it is recorded by the instrument. To perform this assay, we normally used saturating concentrations of substrates and inhibitors:

- 10 mM glutamate/10 mM malate to induce NADH dehydrogenase (complex I) - driven respiration
- 10 mM succinate to induce succinate dehydrogenase (complex II)- driven respiration
- 0.5 mM ADP to induce ATP synthesis (state 3 respiration)
- 6 µg/ml rotenone to inhibit complex I, used together with succinate
- 1.8 mM malonate to inhibit complex II, used together with glutamate/malate
- 60 µM DNP (dinitrophenol) to uncouple the oxidative phosphorylation process

The experiments were carried out as follows: cells were detached from the Petri dishes with trypsin and washed in Hank's buffer and then suspended. An aliquot of cells was loaded in the electrode chamber and diluted in 0.25 M sucrose, 20 mM Tris HCl, 4 mM $MgSO_4$, 0.5 mM EDTA, 10 mM KH_2PO_4 pH 7.4. Cells were immediately permeabilized with 60 µg/ml digitonin at 30°C, and glutamate/malate (plus malonate) or succinate (plus rotenone) were added immediately. State 3 and uncoupled respiration rates were measured in the presence of ADP or DNP (dinitrophenol) respectively. The oxygen consumption rate was observed in the graph as a decrease of oxygen concentration in the electrode chamber over time. It was normalized referring the oxygen consumption rate to the amount of protein measured by the Lowry method, and it was expressed as nmol/min/mg of protein.

3.10 Ca^{2+} signalling measurements

Cytosolic-free Ca^{2+} levels in live cells were measured with the red-fluorescent ratiometric Ca^{2+} indicator Fura-2, AM. At low concentrations of the indicator, 340/380nm excitation ratio allows accurate measurements of the intracellular concentration of the divalent cation. After 24-36h of transfection, cells were loaded with 5mM Fura-2, AM dissolved in fluorobrite DMEM, pH 7.4 (Thermo Fischer Scientific) for 30 minutes. The loading solution was then removed, and cells were washed three times with the same medium. Each cover slip of cells was assembled into a purpose-built chamber and a fresh aliquot of medium was added to the cells and placed on the stage of a Nikon Eclipse Inverted fluorescent microscope equipped with a UV lamp. Cells loaded with the indicator were excited by both 340 and 380 nm wavelengths and live changes were followed after adding 1µM Thapsigargin (Tg), an important SERCA pumps inhibitor. Differences of increasing cytosolic Ca^{2+} concentration among the cell lines could be detected with an increased 340 nm-derived emission light and a decreased 380 nm-derived emission light (increased 340/380 nm). Acquired traces were analysed with Andor iQ live Cell Imaging software.

Mitochondrial Ca^{2+} levels were measured by transfecting the cells with the genetically encoded mitochondrion targeting 4mtGCAMP6 probe, one of the last generation GCamP probes (131). 4mtGCAMP6 is a ratiometric probe, excited by both 475 and 410 nm wavelengths and characterized by a high Ca^{2+} affinity. Recent studies have shown that the GCamP fluorophore has an isosbestic point (410 nm) in its excitation spectrum and exciting GCaMP6m at 410 nm leads to fluorescence emission which is not Ca^{2+} dependent. As a consequence, the ratio between 475 and 410 nm excitation wavelengths is proportional to Ca^{2+} concentration while independent on probe expression levels. The transfection was achieved by using Lipofectamine p3000 as previously described and after 24-36 h of transfection cells were expressing the indicator. The growing medium was then removed and replaced with fresh fluorobrite DMEM, and each cover slip of cells was assembled into a purpose-built chamber and placed on the stage of a Nikon Eclipse Inverted fluorescent microscope, as described above. Cells expressing the indicator were excited at 475 and 410 nm and increasing fluorescence was observed after adding 1µM Thapsigargin (Tg). Traces were acquired and analysed with Andor iQ live Cell Imaging software.

3.11 Protein quantification with the Lowry method (132)

The Lowry method allows the determination of the correct protein amount in the examined sample. It is based on the measurement of the aromatic groups through a colorimetric reaction recorded spectrophotometrically at 750 nm wavelength. It is first necessary to realize a calibration curve with standard albumin (BSA – Sigma Aldrich) before starting the assay: increasing amounts of BSA are prepared from a stock solution of the protein and tested at 278 nm wavelength. The concentration of BSA is extrapolated from the graph according to the measured absorptions related to each BSA aliquot and to the known 1 mg/ml BSA absorption (0.64). Once obtained the calibration curve, the assay is carried out as follows: cells are trypsinized and washed deeply in order to remove all the interfering elements contained in the medium, such as FBS and amino acids. 10% deoxycholate (DOC), H_2O and a misture of NaOH, Na-K tartrate and $CuSO_4$ (100:1:1) are then added to the cells and the suspension is incubated for 10 minutes. Right afterwards, the suspension of cells is supplemented with Folin-Ciocalteau's reagent and left 30 minutes far from light at room temperature. The absorption (Abs) is measured right after. Sample's protein concentration (mg/ml) is calculated applying Lambert-Beer Law and it's referred to the calibration curve previously prepared.

4 RESULTS

4.1 Role played by IF_1 in Ca^{2+} homeostasis regulation

As previously introduced, intracellular Ca^{2+} levels must be tightly controlled to maintain cytosolic Ca^{2+} concentration within the physiological range. Impaired cytosolic Ca^{2+} regulation often leads to cellular dysfunctions and can induce the activation of cell death mechanisms. For this reason, cells have developed many ways of maintaining Ca^{2+} homeostasis by extruding, chelating, or compartmenting the cation. Together with the endoplasmic reticulum, mitochondria play a pivotal role in the intracellular compartmentalization of Ca^{2+}. Increases of mitochondrial Ca^{2+} concentration regulate the increase of ATP synthesis. Recently, a putative binding site for calmodulin in F_1F_O-ATPase IF_1 sequence has been uncovered (46), suggesting that IF_1 may contribute to the regulation of Ca^{2+} level in the intracellular environment. Taking these aspects into account, we set up a campaign of experiments in order to clarify whether IF_1 is involved in mitochondrial Ca^{2+} handling. All the experiments were carried out in scrambled (Scr), and permanently IF_1-knockdown (IF_1 KD) HeLa cells, which were obtained by shRNA interference. Scr cells were used as control and expressed normal levels of the protein of interest.

4.1.1 Cytosolic Ca^{2+} evaluation

Cytosolic Ca^{2+} concentration was the first parameter to be analysed, in order to assess the possible differences between control and IF_1 KD HeLa cells. Cells were incubated with the ratiometric Ca^{2+} indicator Fura-2 for 30 minutes and then imaged with the Nikon Eclipse fluorescent microscope upon pharmacological stimulation with 1µM Thapsigargin (*Tg*), an inhibitor of sarco-endoplasmic reticulum Ca^{2+}-ATPase (SERCA) pumps that blocks the physiological Ca^{2+} reuptake into the ER. As we can see in the graph [Fig.14], Fura-2 ratio increased in both Scr and IF_1 KD HeLa cells after Tg challenge, indicating a quick progressive release of Ca^{2+} from the ER into the cytosol. After the initial rise, cytosolic Ca^{2+} levels then reached a plateau phase. The histograms show the plateau values reached by the cell lines, following ER emptying. Interestingly, IF_1 KD HeLa cells showed a significantly lower

cytosolic Ca^{2+} increase (-40/50%) with respect to controls, suggesting that the ER Ca^{2+} storage capacity is negatively affected by the removal of IF_1-expression.

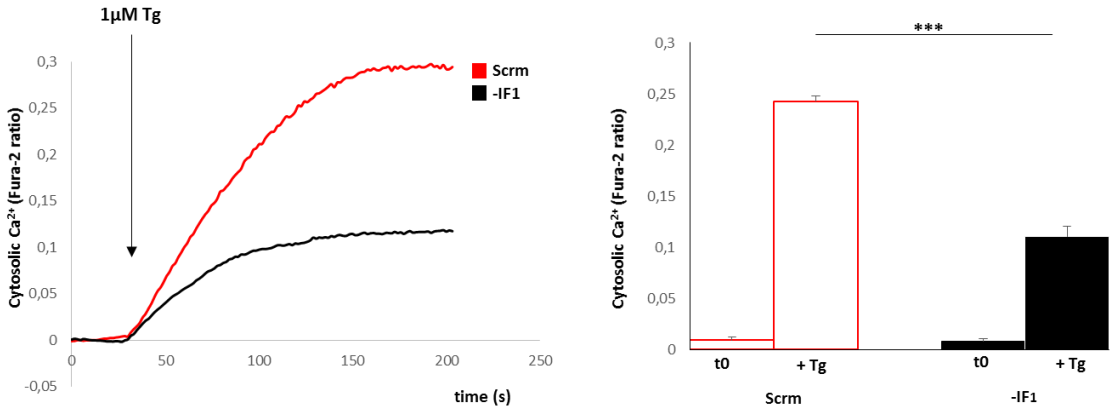

Fig.14. Cytosolic Ca^{2+} increase in Scr (red trace) and IF_1 KD (black trace) cells, upon induction with 1µM Thapsigargin (Tg). On the right: histograms of the plateau values reached by the cell lines once the ER is emptied. IF_1-lacking cells show a significantly lower plateau value (-40/50%). *** $p < 0.001$ indicates the statistical significance with respect to Scr cells.

In order to fully understand whether the modulation of cytosolic Ca^{2+} homeostasis was only related to changes in IF_1 expression or also influenced by IF_1 activation, cytosolic Ca^{2+} response was evaluated in wild type HeLa cells, transiently transfected with either the yellow fluorescent protein (YFP), YFP-IF_1, or YFP-H49P cDNAs. YFP transfected cells were used as control and expressed normal levels of the protein of interest. Cells were instead transfected with YFP-IF_1 to up-regulate IF_1 expression, or with IF_1^{H49P} to induce a higher level of activation. The substitution of His 49 with Pro leads to a change in the pH sensitivity of IF_1 activating the protein even at physiological mitochondrial matrix pH. A similar mutation is reported in (133). Approximately 72 h after the transfection, cells were incubated for 30 minutes with Fura-2 and then immediately analysed. First, 15-20 regions of interest (ROIs) corresponding to transfected, YFP positive, cells were selected, and then ER emptying was induced by adding 1µM Tg to the recording medium. The increase in Fura-2 ratio, which gives a direct indication of the cytosolic Ca^{2+} concentration, were monitored and recorded in all clones. As we could observe, higher cytosolic Ca^{2+} increases were measured in both +IF_1 and IF_1^{H49P} clones (+50%) with respect to control cells, suggesting that the ER Ca^{2+} storage capacity may not only be related to IF_1 up-regulation but also to constitutive activation due to H49P mutation [Fig.15].

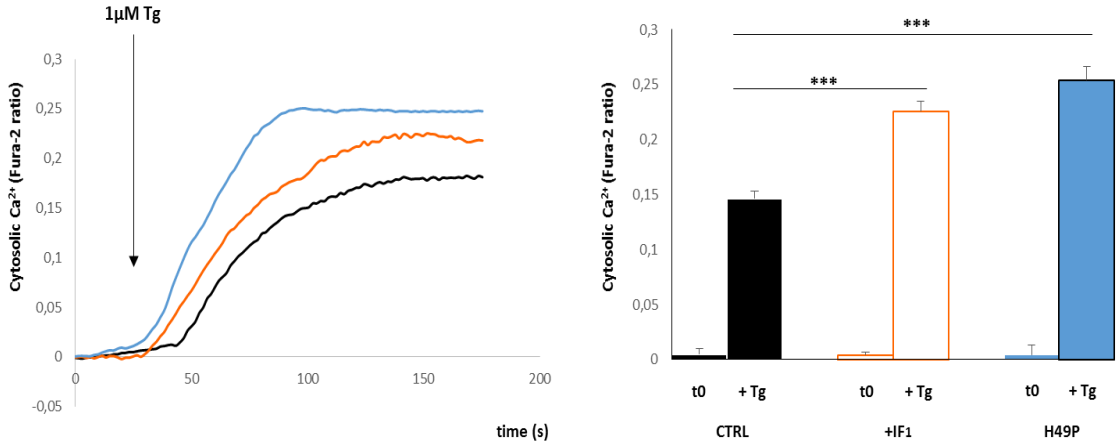

Fig.15. Cytosolic Ca^{2+} increase in control (black), + IF_1 (orange) and IF_1^{H49P} (blue) cells, upon stimulation with 1µM Thapsigargin (Tg). On the right: histograms of the plateau values reached by the clones. Both IF_1 overexpression and constitutively activation are responsible for a different ER's emptying ability. *** $p < 0.001$ indicates the statistical significance with respect to Scr cells

4.1.2 Mitochondrial Ca^{2+} measurements

Considering the presence of statistically significant differences in Tg-induced cytosolic Ca^{2+} accumulation between the genotypes analysed, mitochondrial Ca^{2+} concentration was evaluated in both Scr and IF_1 KD HeLa cells. As fully described in Materials and Methods, cells were transiently transfected with the genetically encoded mitochondrially targeted 4mtGCAMP6 probe. This is a ratiometric probe, excited by 410 and 475 nm wavelengths with a high affinity for Ca^{2+}. The 475/410 nm excitation ratio allows accurate measurements of mitochondrial Ca^{2+} concentration.

After 72 h from the transfection, Ca^{2+} release from the ER was induced with 1µM Tg and changes in mitochondrial Ca^{2+} were monitored with the Nikon Eclipse Inverted fluorescent microscope. Considering the close proximity of mitochondria to the ER, mitochondrial Ca^{2+} variations could be rapidly observed. In this case, a higher increase -and a consequently higher plateau value- in mitochondrial Ca^{2+} concentration occurred in IF_1 KD HeLa cells (+30%) [Fig.16]. This partially explains the lower cytosolic Ca^{2+} increase that was observed in the same cell line.

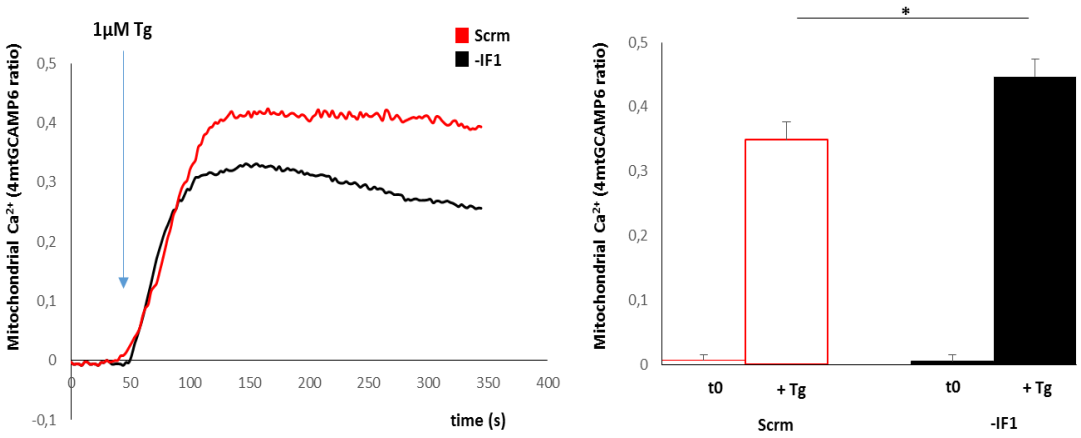

Fig.16. Mitochondrial Ca^{2+} measurement in Scr (red) and IF_1 KD HeLa cells, upon stimulation with 1µM Tg. On the right: histograms of the plateau values reached by the cell lines. * $p < 0.05$ indicates the statistical significance with respect to Scr cells

Mitochondrial Ca^{2+} evaluation was also carried out in wild type control, $+IF_1$ and IF_1^{H49P} cells, but no statistically significant differences were detected among the clones. This might have been caused by performance limitations due to the necessity of co-transfecting the cells with two plasmids.

4.1.3 Mitochondrial Ca^{2+} uniporter (MCU) expression levels in Scr and IF_1 KD HeLa cells

The preliminary data on cytosolic and mitochondrial Ca^{2+} measurements in Scr and IF_1 KD HeLa cells prompted us to analyse the steady state expression levels of the main transporter involved in mitochondrial Ca^{2+} uptake, MCU [Fig.17]. As previously introduced, MCU is a Ca^{2+} sensitive uniporter that resides on the inner mitochondrial membrane and is activated only when the concentration of this cation is high. Its activity is also driven by the mitochondrial membrane potential ($\Delta\psi_m$). MCU expression level was analysed together with VDAC level, another important ion carrier, and the values were normalized to those of ATP synthase (β-subunit) and β-actin, which were used as mitochondrial and cellular loading controls, respectively.

The image shows a significantly increased expression level of MCU in IF_1 KD HeLa cells with respect to Scr cells. This data is in line with the higher mitochondrial Ca^{2+} uptake observed when IF_1 is down-regulated, whereas VDAC level remained unchanged. The histogram shows the quantification of MCU band density relative to β-actin.

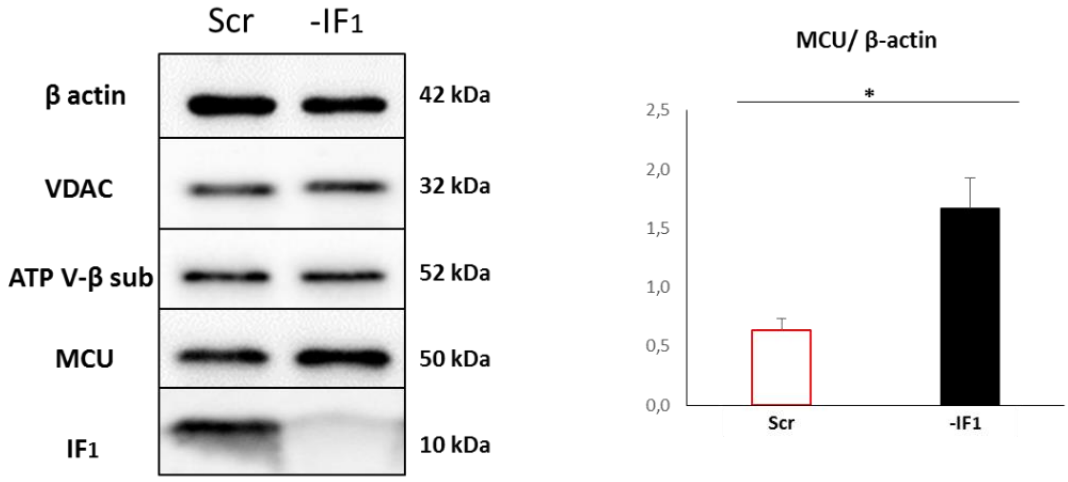

Fig.17. On the left, immunoblot of MCU expression levels in Scr and IF_1 KD HeLa cells. On the right, semiquantitative analysis of MCU levels normalized to β-actin.

Considering these data, the higher mitochondrial Ca^{2+} uptake observed in IF_1 KD cells could be explained by either the higher expression of MCU, or the higher $\Delta\psi_m$ that characterize IF_1 KD HeLa cells (56), Nevertheless, it remains unclear whether MCU overexpression is a pre- or post- transcriptional event and whether IF_1 can actively influence MCU expression and mitochondrial Ca^{2+} uptake via calmodulin regulation. Further analysis of intracellular Ca^{2+} signalling in the presence or absence of IF_1 will therefore be carried out. However, considering the important role of $\Delta\psi_m$ in the maintenance of cellular homeostasis, we decided to carry out a new set of experiments to study and clarify the importance of IF_1 in the regulation of mitochondrial functions in tumor cells.

4.2 143B cell line bioenergetics modulation by IF_1

As reported in literature, IF_1 is overexpressed in many human carcinomas (49) (51). Even if its main activity is considered related to a decrease of mitochondrial matrix pH caused by a collapse of $\Delta\psi_m$, as it occurs in ischemia, its role in tumor cells growing in a physiological environment has been marginally considered. To assess this important aspect, we stably silenced IF_1 expression in human osteosarcoma (143B) cell line and tried to elucidate the importance of the protein in the intracellular bioenergetics modulation.

4.2.1 Screening of IF_1 silencing plasmids in 143B cells

Four different plasmids complementary to the target sequence of human IF_1 mRNA were screened and verified by Western Blotting technique, in order to identify the shRNA sequence with the most efficient IF_1 silencing competence. In addition, a plasmid with a scrambled sequence was used as control of transfection treatment. Comparing the results coming from SDS-PAGE and Western Blotting, plasmid #4 was the most efficient at silencing the protein [Fig.18, A]. The transfection efficiency was also confirmed by bright field and fluorescence microscopy images. In fact, both Scr and #4 plasmids showed an efficient fluorescence intensity (around 30%) proved by the expression of the Green Fluorescent Protein (GFP) [Fig. 18, B]

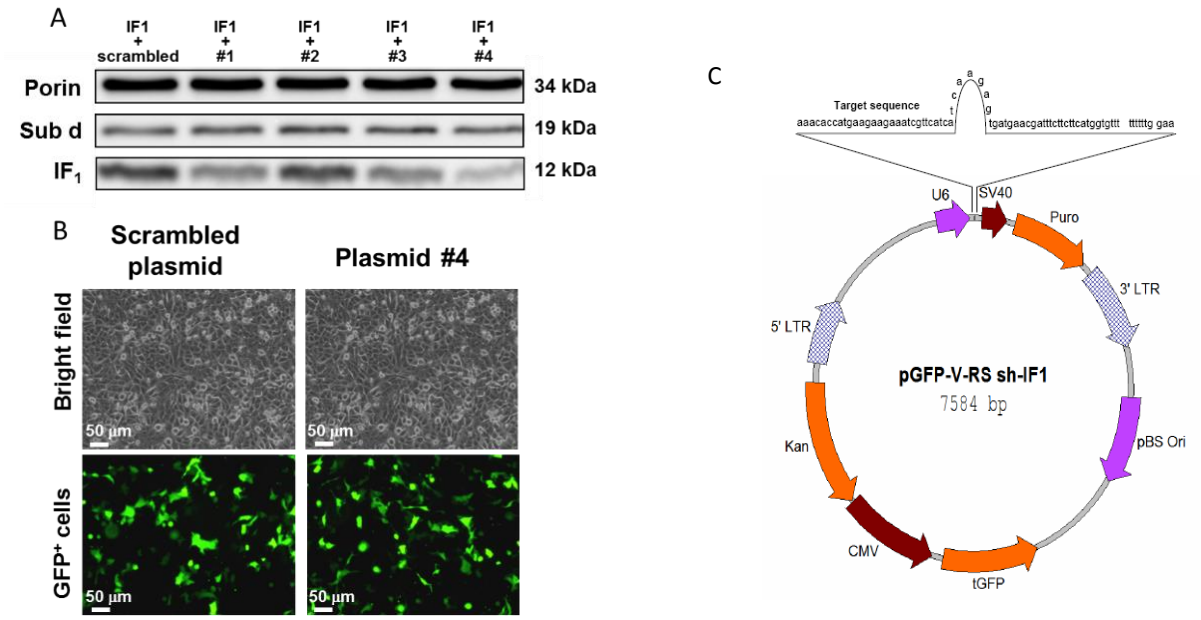

Fig.18. Initial screening of shRNAs for IF_1 silencing. *Panel A*: SDS-PAGE and Western Blotting of Scr and IF_1 silencing plasmids. *Panel B*: bright field and fluorescence microscopy images of Scr and #4 plasmids showing the transfection efficiency. *Panel C*: map of plasmid #4 showing the complete sequence of the construct.

At a later stage, GFP+ single cells resulting from the previous experiments were subcloned and selected with puromycin treatment. Following the selection, the cells were screened once again through SDS-PAGE and Western Blotting analysis. As it is shown in the picture, A7 and D9 clones exhibited the best silencing efficiency, which is still on after 3 years [Fig.19, A].

Transfection stability and morphology of Scr and IF_1 KD 143B cells were assessed by both bright field and flow cytometric analysis [Fig. 19, B and C]. We could finally detect that all the transfected clones were characterized by a high and homogeneous fluorescence intensity of GFP (>98%) and that the transfection technique didn't cause any modification in cell morphology. The stable silencing of the protein was periodically checked by performing SDS-PAGE followed by immunodetection with IF_1 antibody.

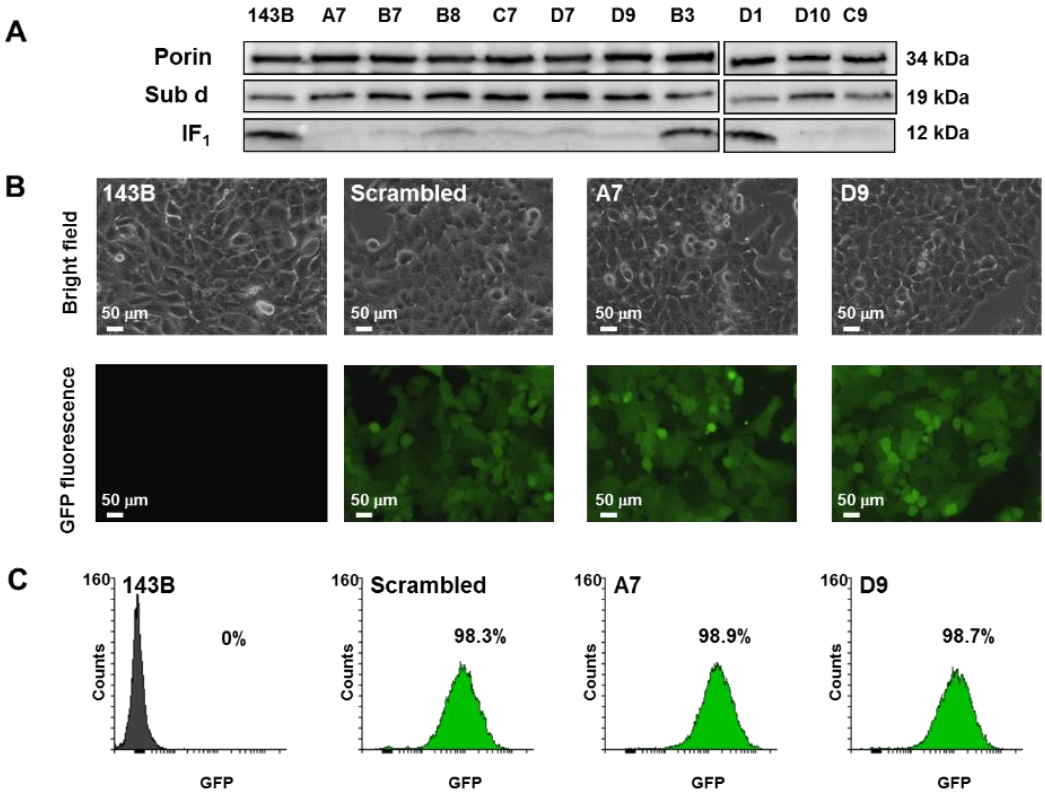

Fig.19. Scr and IF_1 KD clones resulting from subcloning and puromycin selection. *Panel A*: SDS-PAGE and Western Blotting analysis of all obtained clones, using porin and ATP synthase d-subunit as mitochondrial loading controls. *Panel B*: bright field and fluorescence microscopy images showing homogeneous morphology and efficient transfection in all cell clones. *Panel C*: cytofluorimetric quantification of stable transfection efficiency of the chosen Scr and –IF1 clones.

4.2.2 Endogenous mitochondrial membrane potential evaluation in normoxia

Once Scr and stable IF_1-silenced clones were selected for our study, parental, Scr and silenced cells were cultured and seeded for the experiments under normoxic conditions (21% O_2). We

started with the quantification of endogenous mitochondrial membrane potential ($\Delta\psi_m$) in order to evaluate the possible differences in this important mitochondrial function's parameter related to the presence or absence of the protein [Fig.20]. All the cell lines were loaded with 20 nM TMRM for 30 minutes and fluorescence images were obtained by using an inverted fluorescent microscope (x40 magnification): from a first qualitative analysis it could be easily noticed that IF_1-silenced clones showed a higher fluorescence intensity, indicating a higher endogenous $\Delta\psi_m$, when compared with both parental and Scr cells [Fig. 20, A]. A quantitative analysis carried on by using flow cytometry confirmed the qualitative results [Fig. 20, B]. In fact, IF_1-lacking cells showed a significantly higher $\Delta\psi_m$, of around 30%, with respect to IF_1 positive cells. The differences detected among the cell lines were double checked by adding oligomycin, inhibitor of ATP synthase F_o sector, that, as expected, removed all the differences previously observed. This could confirm that the higher $\Delta\psi_m$ obtained in IF_1 silenced clones was attributable to IF_1 absence.

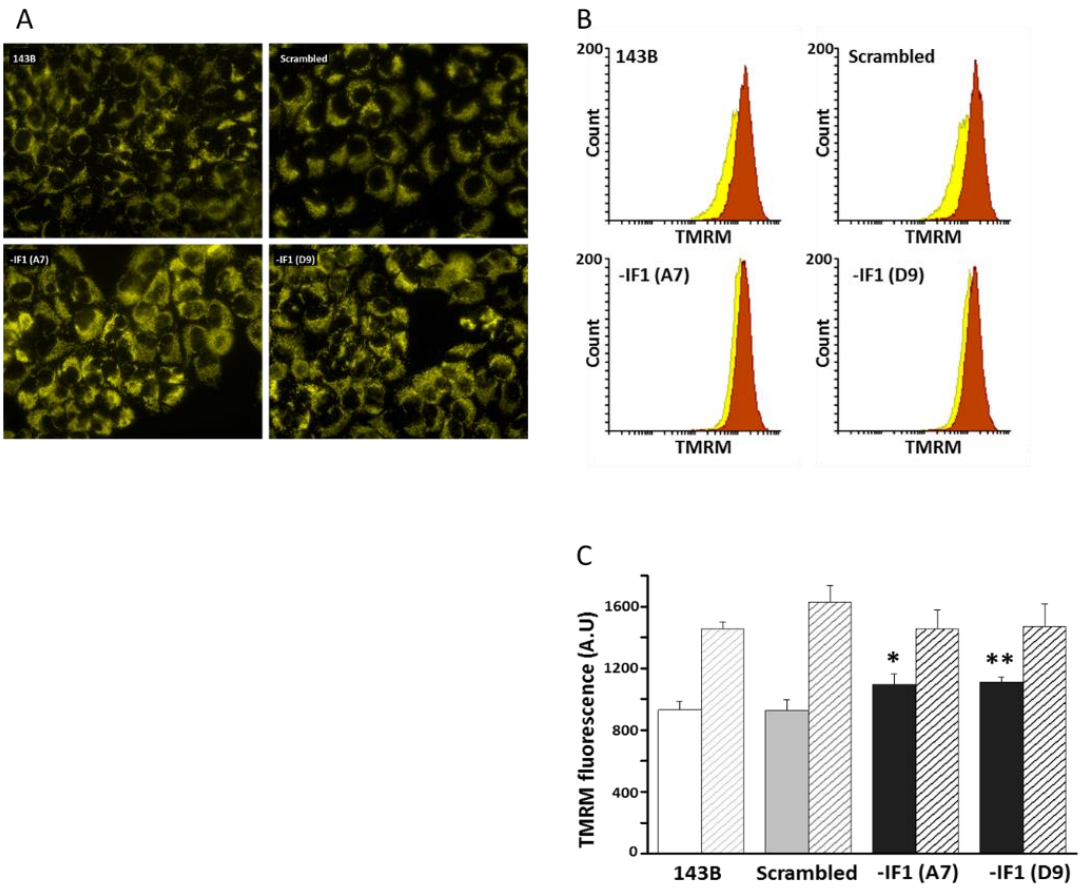

Fig.20. Mitochondrial membrane potential ($\Delta\psi_m$) measurements in parental, Scr and IF_1-silenced 143B cells, loaded with 20 nM TMRM probe. *Panel A*: fluorescent microscopy showing the differences among the cell lines. *Panel B*: flow cytometric analysis of $\Delta\psi_m$ showing a higher endogenous potential in IF_1-silenced cells if compared with controls. *Panel C*: histograms of the semiquantitative evaluations of the obtained results in the absence (filled bars) or in the presence (dashed bars) of oligomycin. ** $p < 0.01$ and * $p < 0.05$ indicate the statistical significance with respect to 143B and Scr cells.

4.2.3 Oxygen consumption rate measurement in normoxia

Intrigued by the results regarding $\Delta\psi_m$, we decided to address the respiratory chain activity by measuring the oxygen consumption rate in all cell lines exposed to normoxia. Cells were washed and loaded in an oxygen Clark-type electrode, as reported by Baracca et al. (128). Following permeabilization with digitonin, 20 mM glutamate/malate (plus malonate) was added to induce Complex I-driven respiration [Fig.21]. State 3 respiration was evaluated by adding saturating concentrations of ADP to maximise ATP synthase's activity. The state 3

oxygen consumption rate increased in all cell lines, and in particular was found slightly, but significantly, lower (-20%) in IF_1-deprived cells if compared with controls [Fig. 21, A and B]. In contrast, no differences were detected among the clones in state 4 respiration induced by adding oligomycin [Fig. 21, A and C].

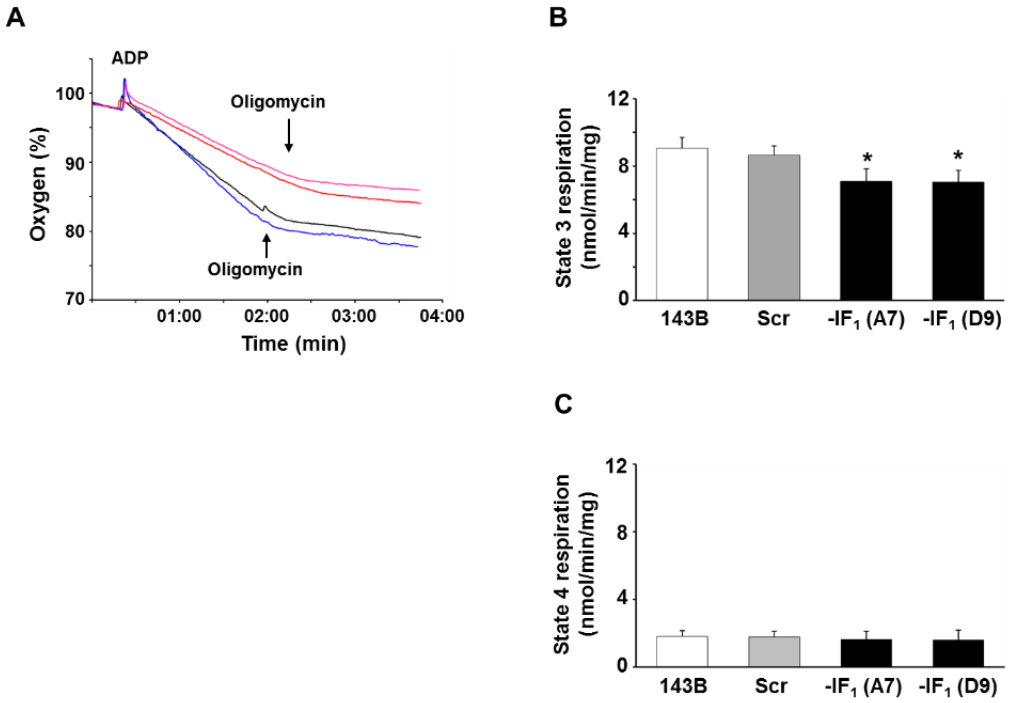

Fig.21. Respiratory chain activity measurement in parental, Scr and IF1-deprived 143B cells. *Panel A*: traces of oxygen consumption rate driven by Complex I, after adding ADP and oligomycin. IF_1-silenced cells (black and blue traces) showed a slight decrease of state 3 respiration of around 20% with respect to controls (red and pink traces). *Panel B*: histograms of state 3 respiration in all cell lines, expressed as nmol/min/mg of protein of consumed oxygen. *Panel C*: histograms of state 4 respiration in all clones (nmol/min/mg of protein). * $p < 0.05$ indicates the statistical significance with respect to 143B and Scr cells.

These results, together with the ones obtained by $\Delta\psi_m$ analysis, suggested that the presence of IF_1 in 143B cell line might enhance the ATP synthesis rate via OXPHOS. Nevertheless, total intracellular ATP content, OXPHOS enzymes expression levels and mitochondrial mass remained unchanged in all cell lines and no detectable differences could be seen (data not shown) (57).

4.2.4 Oligomeric organization of ATP synthase in IF$_1$-silenced clones

Considering the results obtained from $\Delta\psi_m$ and state 3 respiration rate measurements, the oligomeric state of mitochondrial ATP synthase was then investigated under normoxic conditions. To proceed with this study, we first assessed the correct mitochondria extraction method and inner mitochondrial membrane permeabilization, since the type of detergent and its concentration are critical for the execution of the experiment (135). Mitochondria from parental 143B cells were extracted and treated with different digitonin/protein ratios to assess the correct detergent concentration. As we could notice, 2.5/1 digitonin/protein was the best -ATP synthase conservative- condition that could maintain the physiological ATP synthase organization in dimers and monomers, observed through α-subunit immunodetection following first dimension (1D)-Blue Native gel electrophoresis [Fig.22].

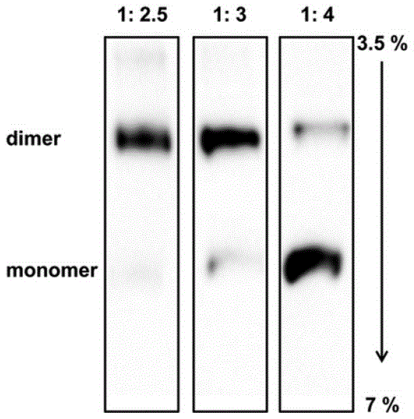

Fig.22. Immunoblot of ATP synthase α-subunit in parental 143B cells showing digitonin/protein titration, performed to evaluate the best condition for oligomeric ATP synthase conservation.

Later on, ATP synthase oligomeric distribution was analysed in all cell lines. Once mitochondria were extracted, BN-PAGE electrophoresis was conducted to separate ATP synthase oligomers and 1D gels were obtained [Fig. 23]. As we can observe in the picture, in-gel ATPase activity was run as control for ATP synthase dimers and monomers localization on the gel. It could be clearly seen that both monomers and dimers exert ATP hydrolytic activity [Fig. 23, A]. The images coming from α-subunit immunodetection showed that the pattern of distribution of the ATP synthase oligomers is the same in parental, Scr and IF$_1$-silenced clones (53-58% monomeric form and 42-47% dimeric form) indicating that the oligomeric distribution of the enzyme is independent from IF$_1$ expression in osteosarcoma cells [Fig. 23, B and D]. Interestingly, the immunodetection of the inhibitor protein showed that when IF$_1$ is present (in

parental and Scr cells), its main target is represented by the dimeric form of the ATP synthase [Fig. 23, C] (57).

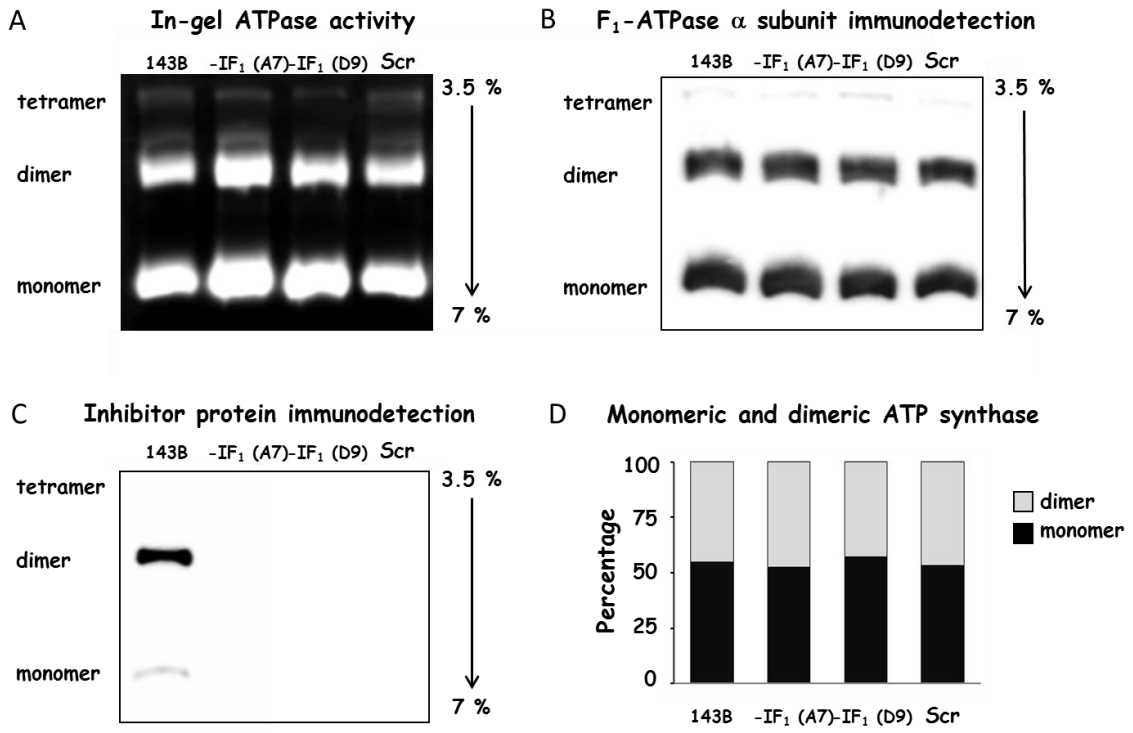

Fig.23. Oligomeric distribution of ATP synthase in parental, Scr and IF_1-silenced 143B cells in normoxia. *Panel A*: in-gel ATPase activity of all cell lines. *Panel B*: α-subunit immunodetection following BN-PAGE electrophoresis that shows the pattern of organization of ATP synthase's oligomers. IF_1 positive and negative cells showed the same distribution of monomers and dimers. *Panel C*: IF_1 immunodetection in all cell lines that shows the IF_1 localization on the dimeric form of the enzyme. *Panel D*: semiquantitative analysis of monomers and dimers distribution in all cells.

Taken together, the results obtained indicated that IF_1 plays an important role in bioenergetics modulation of 143B cell line: in physiological conditions, IF_1 doesn't affect the oligomeric organization of the ATP synthase, but stabilizes the dimeric form of the enzyme, possibly contributing to the enhancing of ATP synthase activity, confirmed by both lower $\Delta\psi_m$ and higher state 3 respiration rate in IF_1 positive cells.

We therefore investigated mitochondrial function changes in the presence or absence of the inhibitor protein under hypoxic exposure, trying to reproduce the hypoxic/anoxic environment occurring in the most central zones of the solid tumor.

4.3 Mitochondrial function regulation in hypoxia

To verify the involvement of IF_1 in cellular and mitochondrial function maintenance we studied the effect of the inhibitor protein under stressing conditions: for this purpose, we performed a new set of experiments on all the cell lines exposed to 0.5% O_2.

4.3.1 IF_1 expression levels in hypoxia

We first evaluated IF_1 expression levels in parental, Scr and IF_1-silenced cells exposed to 24 and 48 h of hypoxia created by an Invivo2 hypoxic chamber. As we could notice, in IF_1-expressing cells a significant increase of the protein expression could be detected through SDS-PAGE followed by Western Blotting. In particular, the semiquantitative analysis of IF_1 level normalized to the β-actin and the ATP synthase α-subunit showed that in both parental and Scr cells the increase was around 50% after 24 h, whereas it was of about 70% after 48 h [Fig.24].

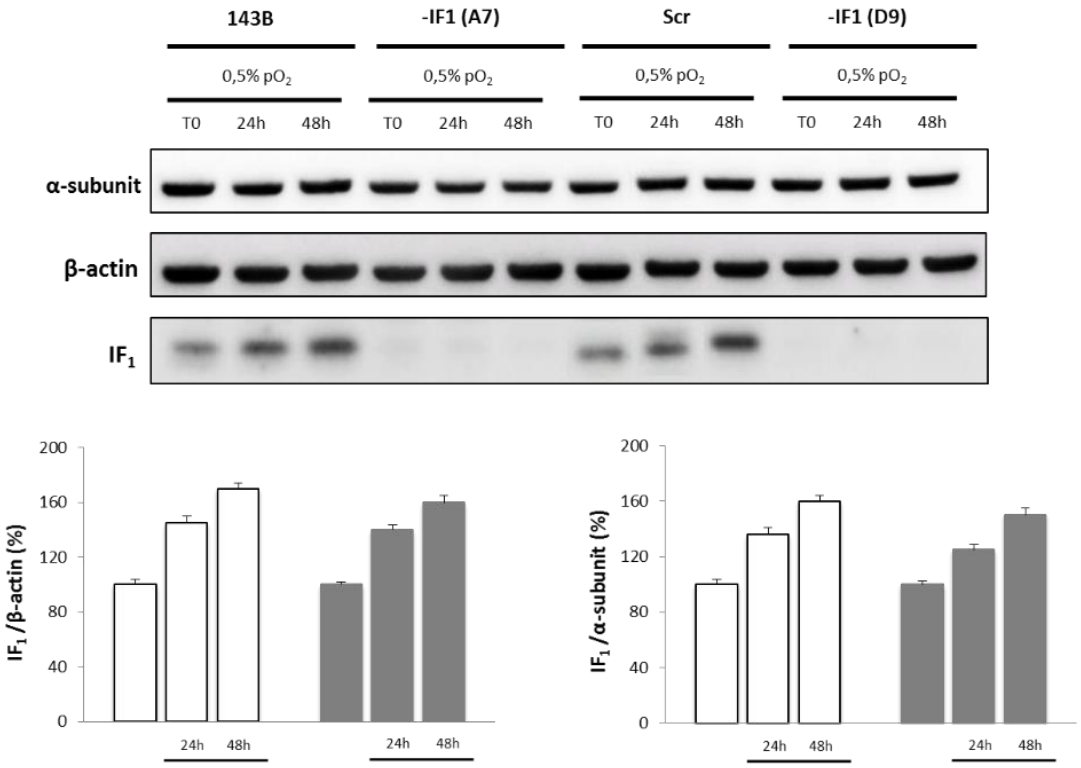

Fig.24. ATP synthase IF_1 expression level analysis in parental, Scr and IF_1-silenced clones obtained through SDS-PAGE and Western Blotting. Both parental and Scr cells showed a progressive increase of IF_1 levels in hypoxia.

4.3.2 Cell growth

Considering the results obtained regarding IF_1 content, cells proliferation ability was tested in all cell clones. Cells were exposed to hypoxia up to 72 h and the growth rate was measured every 24 h. As we can observe from the graph, IF_1-silenced cells showed a significant decrease of proliferation rate after 48 h, with respect to parental and Scr cells, which instead maintained an efficient replication activity even after 72 h from the seeding. The cell growth traces suggested that IF_1 absence might contribute to a more difficult cell adaptation to hypoxia [Fig. 25].

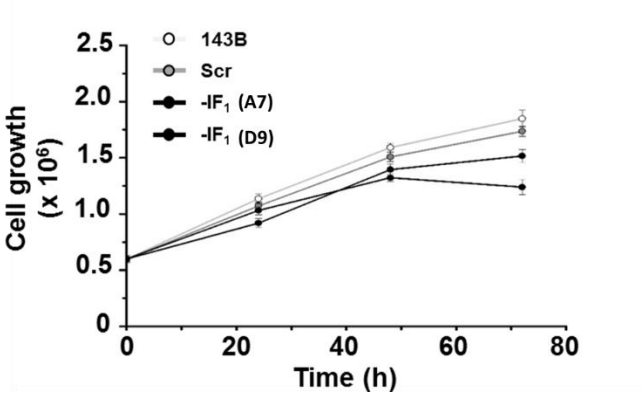

Fig.25. Cell growth evaluation of parental, Scr (grey traces) and IF1-silenced (black traces) 143B cells under hypoxic exposure (0.5% O_2)

4.3.3 Mitochondrial membrane potential evaluation in hypoxia

Considering the increased IF_1 levels and the different proliferation rate observed in hypoxia, we decided to investigate the effects of IF_1 up-regulation on $\Delta\psi_m$. Cells were exposed to 0.5% O_2 for 24 h and then loaded with 20 nM TMRM probe for 30 minutes. Images obtained through fluorescence microscopy showed a high $\Delta\psi_m$ in both parental and A7 clones [Fig. 26, A]. This qualitative observation was confirmed by flow cytometric analysis of $\Delta\psi_m$ in all cell lines, where no differences could be detected in the presence or absence of IF_1 [Fig. 26, B]. In particular, $\Delta\psi_m$ was found to be increased in IF_1-expressing cells with respect to normoxia (see previous results), suggesting that the lower concentration of oxygen is probably responsible for a slowdown in the ETC activity. Since no differences concerning $\Delta\psi_m$ could be detected in the

presence or absence of IF_1, we concluded that probably in these conditions, mitochondria were not sufficiently depolarized to induce ATP hydrolysis.

A slight increase of $\Delta\psi_m$ was then induced by adding oligomycin, indicating that in the examined conditions $\Delta\psi_m$ was very close to state 4 of respiration [Fig. 26, C].

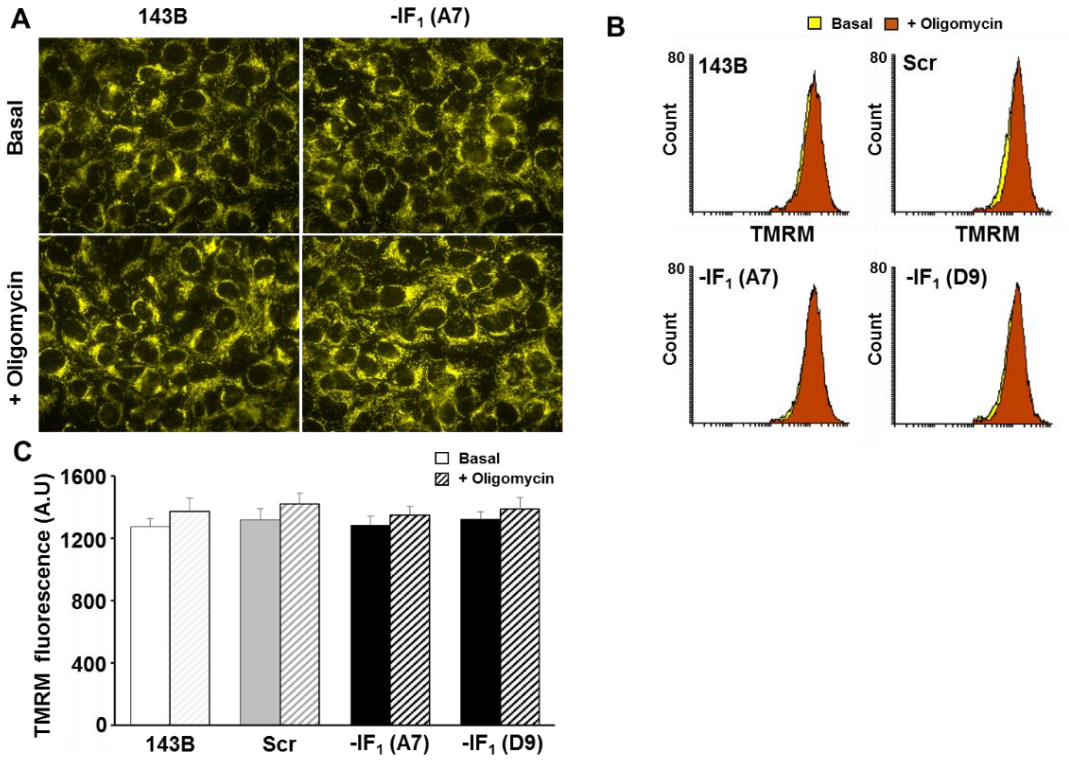

Fig.26. Mitochondrial membrane potential ($\Delta\psi_m$) measurements in parental, Scr and IF_1-silenced 143B cells exposed to 24 h of hypoxia. *Panel A*: fluorescent microscopy images showing a high $\Delta\psi_m$ in both parental and A7 (-IF_1) clones. *Panel B*: flow cytometric analysis of $\Delta\psi_m$ where no differences could be detected among the cell lines. *Panel C*: histograms of the semiquantitative analysis of $\Delta\psi_m$ in the absence (filled bars) or in the presence (dashed bars) of oligomycin.

4.3.4 Mitochondrial mass evaluation

Mitochondrial membrane potential measurements are strictly dependent on mitochondrial mass content, especially when fluorescent probes are used, since a different signal in the fluorescence intensity may be recorded according to the number of mitochondria analysed. For this reason, a mitochondrial mass check needed to be run. After 24 h of hypoxic exposure, cells were collected and permeabilized and citrate synthase activity assay was carried out [Fig.27]. The

results, expressed as nmol/min/mg of protein, showed that citrate synthase activity was the same in all cell clones (dashed bars) and a slight decrease (around -15%) was observed with respect to normoxia (filled bars).

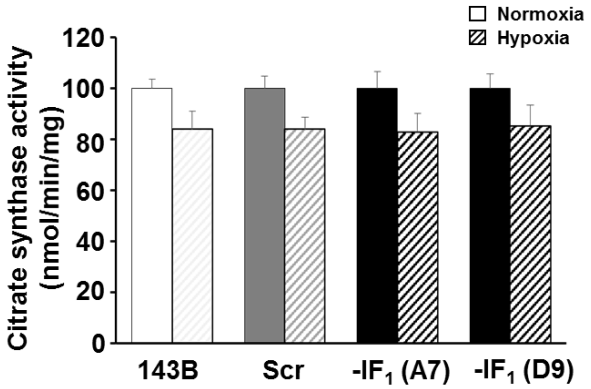

Fig.27. Mitochondrial mass analysis of all cell lines through citrate synthase activity assay (nmol/min/mg of protein). No differences were detected among the clones either in normoxia or in hypoxia.

4.3.5 Glucose consumption and lactate release

In order to confirm that no ATP hydrolysis had been activated in our experimental conditions, the glycolysis efficiency was tested by measuring glucose consumption and lactate release. Cells were exposed to 24 h of hypoxia and media were then collected for the assay. As expected, no significant difference could be detected among the cell lines, concerning either glucose consumption, or lactate production, both expressed as µmol/10^6 cells. In addition, lactate release/glucose consumption ratio was found to be 2/1 in all clones, indicating that all consumed glucose was converted into lactate, independently from the presence of IF_1 [Fig. 28].

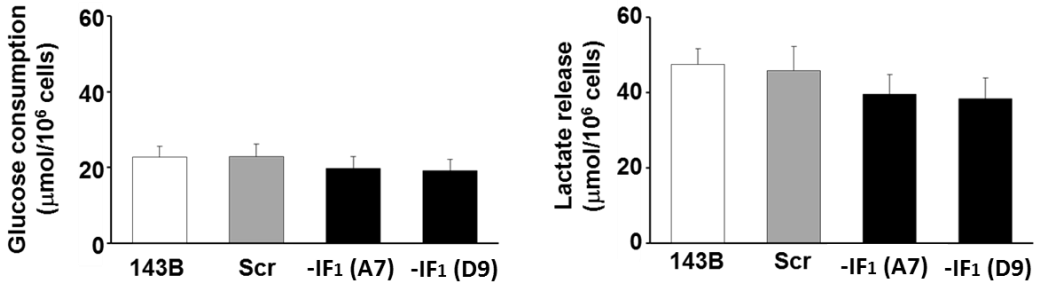

Fig.28. Glucose consumption (μmol/10^6 cells) on the left, and lactate release (μmol/10^6 cells) on the right, of parental, Scr and IF_1-non expressing cells in hypoxia. No significant differences were detected among the cell lines.

4.3.6 Steady state ATP level

The study was continued with the total steady state ATP content measurement in all cell lines. Cells were left for 24 h in the hypoxic chamber and then permeabilized for the ATP quantification through luminometric assay. Even in this case we could not observe any significant difference in total ATP level among the cell clones [Fig.29].

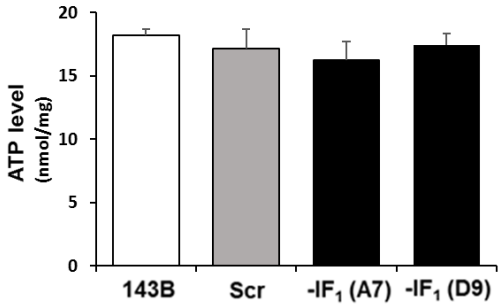

Fig.29. Steady state ATP level (nmol/mg of protein) in all cell lines exposed to 0.5% O_2 remained unchanged.

4.3.7 OXPHOS enzymes expression levels analysis

Trying to find an explanation to the high $\Delta\psi_m$ found in hypoxia in all cell lines, we assessed the OXPHOS complexes expression levels in all cell lines. 143B cells were seeded and exposed for 24 h to hypoxia and then collected and lysed to perform SDS-PAGE. Following the electrophoresis run, the proteins were immediately blotted onto a nitrocellulose membrane and

incubated with a cocktail of antibodies anti-OXPHOS complexes. As we can see in the image, a detectable difference could be observed in complex I expression: both IF_1 expressing and non-expressing cells showed significantly higher levels (+70/80%) of the complex if compared to normoxia [Fig. 30]. A slight, but significant, increase (+15%) of complex II was detected as well.

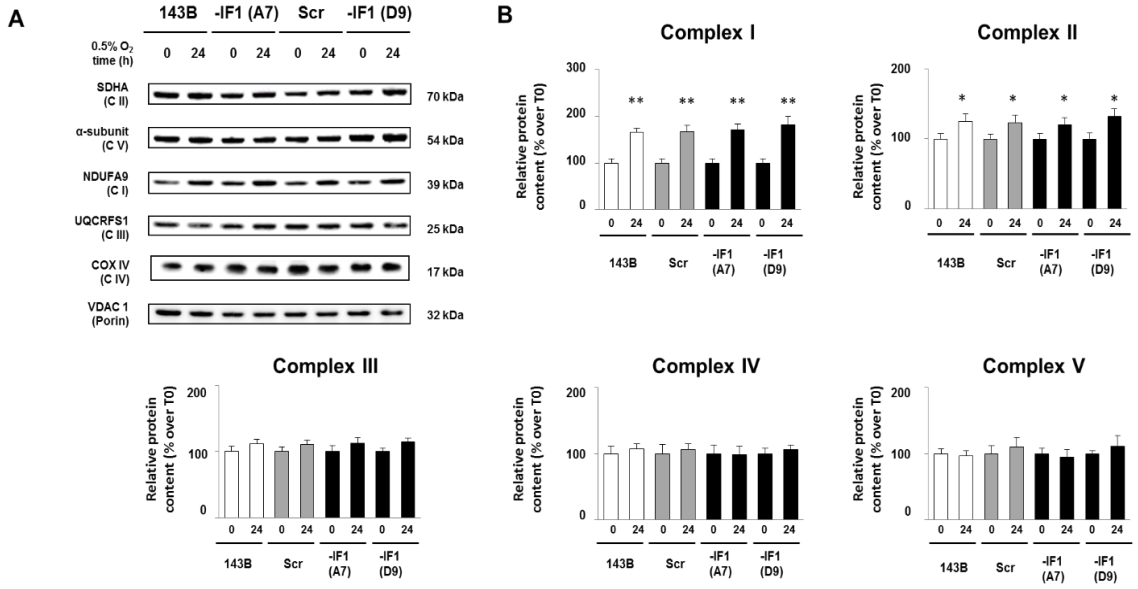

Fig.30. Immunodetection of OXPHOS complexes in parental, Scr, and IF_1-silenced cells exposed to 24h of hypoxia (0.5% O_2). The quantification of the protein content was normalized to the porin, taken as mitochondrial loading control. Complex I was found to be significantly increased (+70%, **p<0.01) in all cell lines exposed to hypoxia with respect to normoxia. A slight significant increase (+15/20%, *p<0.05) was also found in complex II expression level.

Overall, the data obtained so far led us to conclude that probably the oxygen tension in use was not sufficient to induce a complete depolarization of the mitochondrion, necessary for ATP hydrolysis activation and glucose consumption increase, both fundamental for IF_1 binding to ATP synthase. Further investigation is now on to clarify the effect of the inhibitor protein on mitochondrial and cellular metabolism in chemically induced-stressing conditions.

5 DISCUSSION

Tumor cells exhibit genetic, biochemical and histological differences with respect to non-transformed cells. One of their most important features is the metabolic switch towards glycolysis which leads to a higher glycolytic flux to compensate the increased energy demand (Warburg effect) (5). Indeed, many biochemical mechanisms may contribute to increasing the glycolysis rate, one of which has recently been proposed to be the inhibition of the mitochondrial ATP synthase by the natural inhibitor protein, IF_1 (51). As fully described in the introduction, the importance of IF_1 is related to many intriguing aspects that prompted us to deeply study the involvement of this protein in the regulation of the energetic state of tumor cells. IF_1 is a basic, stable protein of 106 amino acids in humans (136), highly evolutionary conserved among species. Besides the canonical role ascribed to IF_1, its involvement in tumorigenesis has been proposed and studied in the last few years. Interestingly, it has been observed that it is overexpressed in many human carcinomas (51) (49), suggesting a role in cancer cell survival, growth and invasiveness.

It is well established that when the electrochemical proton gradient ($\Delta\psi_m$) across the inner mitochondrial membrane collapses, as it occurs in case of a dramatic mitochondrial respiration impairment, the ATP synthase reverses its activity hydrolysing cytosolic ATP, mostly derived from glycolysis, to restore the intermembrane potential (43) (45). In such condition, either the collapse of $\Delta\psi_m$ or the shift to glycolysis (resulting in an increased lactate production) may contribute to a decrease in the pH leading to the activation of the inhibitor protein (50). Once activated, it binds to the αβ interface of the ATP synthase and blocks the reversal of the enzyme. This fine regulation of ATP hydrolysis by IF_1 is fundamental to prevent massive energy depletion, event that could rapidly lead to cell death. As introduced, the importance of $\Delta\psi_m$ is not only associated with the control of ATP synthesis efficiency, but it is also fundamental for proteins transport, mitochondrial morphology maintenance, cell death regulation, ions homeostasis and ROS production handling.

Considering the important role played by IF_1 in ATP synthase modulation, the first part of this study was dedicated to addressing tumor cells bioenergetics in the presence or absence of the protein under physiological non-stressing conditions. The first step was the evaluation of a possible involvement of IF_1 in mitochondrial Ca^{2+} signalling. Mitochondria are important Ca^{2+} storage sites in the cell, together with the endoplasmic reticulum (ER). Recently, a putative

binding site for calmodulin in IF_1 sequence has been uncovered (46), suggesting that it may contribute to the regulation of Ca^{2+} level in the intracellular environment. For these reasons, scrambled (Scr) and permanently IF_1-knockdown (IF_1 KD) human adenocarcinoma cells (HeLa cells) were used to clarify the possible contribution of IF_1 to mitochondrial Ca^{2+} signalling. The first aspect to be assessed was the cytosolic free-Ca^{2+} content quantification measured by using the ratiometric indicator Fura-2. Thapsigargin (Tg), an important inhibitor of ATP-dependent Ca^{2+} uptake into the ER, was used to induce a hormone-like elevation of cytosolic Ca^{2+}. The results obtained showed that when ER's emptying was stimulated by Tg, an increase in cytosolic Ca^{2+} was recorded in both Scr and IF_1-silenced cells, but in the absence of IF_1 this increase was significantly lower, suggesting that ER's storage capacity is probably higher when IF_1 is present. In order to fully understand whether the differences in cytosolic Ca^{2+} increase were only related to IF_1 expression levels or they could be even associated to IF_1 activation, the same experiment was conducted in wild type HeLa cells, transiently transfected with either yellow fluorescent protein (YFP), or YFP-IF_1, or YFP-H49P plasmids. YFP cells were used as control of transfection and expressed normal levels of IF_1. Instead, in YFP-IF_1 cells a genic up-regulation of IF_1 was induced, whereas IF_1^{H49P} cells carried a mutation in His 49. The latter was obtained by substituting His with Pro, leading to a changing in IF_1's pH sensitivity and making it active even at physiological pH (constitutive activation). Interestingly, cytosolic Ca^{2+} increase upon stimulation with Tg was significantly higher in both IF_1 overexpressing and constitutively active clones with respect to YFP controls, indicating that either IF_1 expression levels or constitutively activation of the protein may play a role in cytosolic Ca^{2+} response to Tg. Given the close proximity of the ER to the mitochondria, we decided to investigate the cross-talk between the two Ca^{2+} storage compartments in the presence or absence of IF_1. Scr and IF_1 KD HeLa were transiently transfected with the genetically encoded mitochondrion targeting 4mtGCAMP6 probe and after 72 h they were imaged and analysed. In this case, Tg induced a higher increase of mitochondrial Ca^{2+} concentration in IF_1 lacking cells with respect to controls. This result was considered in line with what obtained from the analysis of the cytosolic Ca^{2+} response.

Mitochondrial Ca^{2+} uptake is allowed by specific and non-specific transporters and ion channels situated on the outer and the inner mitochondrial membranes (OMM and IMM, respectively). In particular, although originally thought to be exclusive component of the OMM, it has been then demonstrated that VDAC is located in the contact sites between the OMM and the ER (105). Ca^{2+} transport across the IMM is instead exerted by a rapid electrogenic pathway, the

mitochondrial calcium uniporter (MCU), which quickly transports Ca^{2+} into the matrix, driven by the negative charge of the membrane potential established by the respiratory chain (106). Trying to give an explanation to the results obtained, the main mitochondrial Ca^{2+} transporters expression levels were addressed. The results coming from SDS-PAGE and following Western Blotting showed that VDAC levels remained unchanged between Scr and $-IF_1$ cells, whereas an up-regulation of MCU was observed in IF_1-silenced cells with respect to controls. This result could in part explain the higher mitochondrial uptake of Ca^{2+} in IF_1 KD HeLa cells: an enhanced MCU expression, driven by the negative charge of the $\Delta\psi_m$ found in the mitochondrial matrix of IF_1 KD HeLa cells (56) would be able to induce a higher uptake of Ca^{2+} into the mitochondria. What would be interesting to deepen is whether MCU overexpression is a pre- or post-transcriptional event and whether IF_1 would be able to directly modify MCU levels not only by regulating $\Delta\psi_m$, but also by interacting with calmodulin. Further investigation concerning intracellular Ca^{2+} signalling changes in the presence or absence of IF_1 will be carried out. However, considering the important role of $\Delta\psi_m$ in the cellular homeostasis maintenance, a new campaign of experiments was conducted in order to study and clarify the importance of IF_1 in the regulation of mitochondrial functions in tumor cells.

We stably silenced the expression of the inhibitor protein in human osteosarcoma 143B cell line and to study the possible changes occurring in $\Delta\psi_m$ and bioenergetics. The efficiency of the transient transfection by using the scrambled (Scr) and #4 plasmids was around 30% and upon puromycin selection and subcloning, stably transfected clones were obtained (A7 and D9). The immunodetection with IF_1 antibody showed that the silencing was of around 90-95% compared to parental and Scr cells. The periodic check of IF_1 expression level in silenced clones confirms that the silencing is still present after 3 years. Once Scr and IF_1-silenced clones were selected, parental, Scr and silenced cells were used to evaluate $\Delta\psi_m$ under physiological conditions (normoxia) by using the fluorescent TMRM probe. The increased $\Delta\psi_m$ measured in both A7 and D9 clones with respect to Scr and parental cells matched with the results obtained in HeLa cells (56), suggesting that the presence of IF_1 may contribute to ATP production in normoxia. At the same time, our result was in contrast with what reported by Sanchez-Cenizo et al. (51), who found increased $\Delta\psi_m$ in different carcinoma cells transiently overexpressing IF_1. In this case, it is important to underline that transiently transfected cell populations may represent a heterogeneous system where both transfected and control cells co-exist: such a model wouldn't represent a stable steady state metabolic condition, but a dynamic situation that

could produce potentially ambiguous data. However it can't be excluded that different cell types may behave differently from HeLa or 143B cells.

The steady state $\Delta\psi_m$ level found in 143B cells was double checked with 0.6 µM oligomycin, which, as expected, increased the fluorescence intensity in all cell lines removing all the differences previously detected. This result indicated that the differences observed among parental, Scr and IF_1 KD cells could be ascribed to the presence or absence of the protein and, in addition, that no ATP hydrolysis had been triggered under normoxic conditions: according to recent work (137), when ATP hydrolysis significantly contributes to the maintenance of $\Delta\psi_m$, the addition of oligomycin results in $\Delta\psi_m$ collapse despite the presence of IF_1. Intrigued by these results, the efficiency of the electron transport across the mitochondrial respiratory chain was addressed by measuring the oxygen consumption rate (OCR) in all cell lines exposed to normoxia. The results obtained showed that under ADP phosphorylating conditions (state 3 of respiration) the respiration rate was higher in parental and Scr cells than in IF_1-silenced clones. Even in this case, the addition of oligomycin levelled out the differences among the cell lines by completely blocking the ATP synthase activity. Taken together, $\Delta\psi_m$ analysis and OCR measurement indicated that the presence of the inhibitor protein in 143B cells can enhance the rate of ATP synthesis via OXPHOS and suggested that the absence of IF_1 doesn't have any effect on the respiratory chain activity. Nevertheless, any significant difference was observed concerning OXPHOS expression levels, mitochondrial mass and total ATP content among the cell lines (57).

In the last few years, IF_1 presence has been associated with an enhanced oligomerization level of the ATP synthase: active dimers of IF_1 would bind two F_1 portions coming from two distinct ATP synthase enzymes actively promoting the formation of ATP synthase dimers (47) (58). This process would induce the formation of local curvatures in the inner membrane, the so called *mitochondrial cristae*, generating areas of very high protons concentration and thus increasing the ATP production rate (40). Considering the lower steady state level of $\Delta\psi_m$ and the higher ADP-induced OCR found in both parental and Scr cells, we decided to elucidate the involvement of IF_1 in the oligomeric distribution of the ATP synthase. The first step was to assess the correct protein/detergent concentration in order to maintain the physiological inner membrane complexes distribution: in fact, excess of detergent concentration can dismantle mitochondrial inner membrane's superstructures (135). In particular, the first dimension-gel immunodetection of the ATP synthase's α-subunit showed that the ratio of 1:2.5 (protein/digitonin) was the best at maintaining the actual distribution of the enzyme. After that,

the oligomeric organization of the enzyme was studied in all the cell lines and no differences in the dimers/monomers distribution could be detected in the presence or absence of the inhibitor protein, indicating that in osteosarcoma cell line IF_1 does not promote ATP synthase oligomerization. However, when IF_1 was present, it was completely associated to the dimeric form of the enzyme.

All the results obtained in normoxia lead us to conclude that in human 143B cell line IF_1 does not affect the level of F_1F_O-ATPase oligomerization, even though it possibly stabilizes the dimeric form of the enzyme. The lower $\Delta\psi_m$ and the higher state 3 respiration rate found in IF_1 expressing cells suggested that IF_1 might enhance ATP production via OXPHOS.

The following step was to verify the involvement of IF_1 in cellular and mitochondrial function maintenance under hypoxic exposure, trying to reproduce the hypoxic/anoxic environment occurring in the most central zones of solid tumors. To recall, nutrients and oxygen reach the solid tumor travelling across pre-existing and new-generated blood vessels. When the tumor is growing, the pre-existing vessels may be easily disrupted or damaged and the new capillaries may be characterized by structural abnormalities. These events, together with a possible reduction of the oxygen transport or an increased oxygen consumption by tumor cells, may contribute to the generation of hypoxic areas. The concentration of oxygen in the close proximity of the blood vessels is normally around 2%, but, the larger the distance from the vessels is, the lower the oxygen tension becomes: cells 200 µm far from the capillary endothelium may be even exposed to 0.2% oxygen concentration, creating areas of severe hypoxia/ischemia (66) (67). To verify whether IF_1 may play a role in protecting tumor cells under stressing/hypoxic conditions, we performed a new set of experiments on both IF_1-expressing and non-expressing 143B clones exposed to hypoxia (0.5% O_2).

We started by analysing IF_1 expression changes in parental and Scr cells exposed to the hypoxic environment for 24 and 48 h. Interestingly, we could notice that both parental and Scr cells progressively increased IF_1 content with respect to normoxia. Given this result, the cell growth and proliferation rates were assessed in all cell lines. As we could observe, IF_1-lacking cells slowed down their proliferation rate after 48 h from the seeding, differently from parental and Scr cells, which instead maintained an efficient replication ability even after 72 h, suggesting that when IF_1 is present it may promote a better adaptation to hypoxia. Once IF_1 content and proliferation rate had been verified, we carried on our study analysing 143B's behaviour after 24 h of hypoxia, considering this exposure time sufficient to induce an increased expression of

the protein. The analysis of endogenous $\Delta\psi_m$ in the presence or absence of the inhibitor protein was first performed. Surprisingly, from the microscopy images obtained we could not observe any depolarization of the mitochondria, neither in the presence nor in the absence of IF_1. In particular, flow cytorimetric analysis of endogenous $\Delta\psi_m$ showed that in both parental and Scr cells it was increased with respect to normoxia. The addition of oligomycin further increased $\Delta\psi_m$ in all cell lines, indicating that no ATP hydrolysis was occurring: in fact, if mitochondria had been sufficiently depolarized, we would have expected to observe a very low steady state $\Delta\psi_m$ in all cell lines. In particular, IF_1 non-expressing cells should have showed a slightly higher $\Delta\psi_m$ with respect to parental and Scr cells, due to uncontrolled ATP hydrolysis, and in the presence of oligomycin it should have collapsed as a result of the ATP hydrolytic activity of the F_1F_O-ATPase complex. We concluded that the limited availability of oxygen probably slowed down the electron transport across the inner membrane complexes (less than ATP synthesis by OXPHOS), thus increasing $\Delta\psi_m$.

Moreover, since $\Delta\psi_m$ measurements are strictly dependent on the total number of mitochondria in the cells, an evaluation of mitochondrial mass was carried out by analysing the citrate synthase activity. Citrate synthase is the first enzyme of Kreb's cycle and it is commonly used as mitochondrial matrix marker. The assay was run after 24 h of hypoxia and no differences could be detected among the cell lines, since the slight decrease observed with respect to normoxia was the same independently from the presence of IF_1. This result indicated that the fluorescence intensity exerted by the TMRM probe was not affected by differences in mitochondrial mass.

In order to confirm that ATP hydrolysis had not been triggered in our experimental conditions, we explored the glycolysis efficiency in all cell lines exposed to 24 h of hypoxia. The results obtained showed that any significant difference could be detected among the cell lines, neither in glucose consumption, nor in lactate release, and that all consumed glucose was converted into lactate in all cell lines. This data supported our hypothesis that no ATP hydrolysis occurred in our experimental conditions: in fact, if it had been activated, we would have expected to observe a sharp increase of glucose consumption (and lactate production) in IF_1-silenced cells caused by an uncontrolled energy wasting. In addition, when steady state ATP levels were assessed, we noticed that in the absence of IF_1 they were not decreased as we would have expected if ATP hydrolysis had been activated.

However, intrigued by the high $\Delta\psi_m$ observed in hypoxia, we carried out the quantification the OXPHOS enzymes expression levels in all cell lines exposed to 24 h of hypoxia. Interestingly, the immunodetection of the ETC's complexes showed that no difference could be detected among the clones, except for complex I: in fact it was found to be significantly increased in all cells lines, but independently from IF_1 levels. We might speculate that the higher expression of complex I may contribute to the high $\Delta\psi_m$ maintenance found in hypoxia.

Taken together, the results obtained in hypoxia showed that IF_1 increased its expression after 24 h of hypoxic exposure and that the proliferation rate of IF_1-non expressing cells was significantly lower than in controls, suggesting that in the presence of the protein the cells better adapted to the stressing conditions. However, this event didn't find a confirmation in an impairment of mitochondrial function in the absence of IF_1: neither $\Delta\psi_m$, nor glycolysis and ATP content resulted modified, indicating that our experimental conditions could not induce the transmembrane potential collapse necessary to lower pH and promote IF_1 dimerization and activation to inhibit the F_IF_O-ATPase. For this reason, further investigation is now on in our laboratory to shine light on the role of the inhibitor protein as a modulator of mitochondrial and cellular metabolism in chemically induced-ischemic conditions, by using the uncoupler agent FCCP.

6 Conclusions

In the present study, the role played by the endogenous ATP synthase inhibitor protein, IF_1, in tumor cells was addressed. We went through the evaluation of the possible involvement of IF_1 in mitochondrial Ca^{2+} homeostasis handling, drawing then the attention to the assessment of the role exerted by the protein in the regulation of the metabolic and energetic state of tumor cells under both physiological and stressing conditions.

Summarizing, on the basis of the data so far obtained we can conclude that:

- ✓ In HeLa cells grown in *normoxia*, IF_1 regulates mitochondrial Ca^{2+} uptake by modulating mitochondrial membrane potential-driven MCU expression
- ✓ In 143B cells grown in *normoxia* (21% O_2), IF_1 doesn't affect the oligomeric organization of the ATP synthase but it possibly stabilizes the dimeric form of the enzyme. We suppose that the lower $\Delta\psi_m$ found in both parental and scrambled cells, supported by a higher state 3 respiration rate, is due to a higher ATP production via OXPHOS
- ✓ In 143B cells grown in *hypoxia* (0.5% O_2) the experimental conditions were not sufficient to induce a complete loss of $\Delta\psi_m$, essential for IF_1 to inhibit the F_1F_O-ATPase complex, even though IF_1-expressing cells showed a higher proliferation rate with respect to IF_1-null clones, supporting the notion that IF_1 plays important role(s) in cells exposed to severe hypoxia/anoxia.

Bibliography

1. Wallace DC. Mitochondria and cancer. Nat Rev Cancer. 2012 Oct;12(10):685–98.

2. Zimorski V, Ku C, Martin WF, Gould SB. Endosymbiotic theory for organelle origins. Curr Opin Microbiol. 2014 Dec;22:38–48.

3. John P, Whatley FR. Paracoccus denitrificans and the evolutionary origin of the mitochondrion. Nature. 1975 Apr 10;254(5500):495–8.

4. Farrar GJ, Chadderton N, Kenna PF, Millington-Ward S. Mitochondrial disorders: aetiologies, models systems, and candidate therapies. Trends Genet. 2013 Aug 1;29(8):488–97.

5. Warburg O. On the origin of cancer cells. Science. 1956 Feb 24;123(3191):309–14.

6. Solaini G, Sgarbi G, Baracca A. Oxidative phosphorylation in cancer cells. Biochim Biophys Acta. 2011 Jun;1807(6):534–42.

7. Mathupala SP, Ko YH, Pedersen PL. The Pivotal Roles of Mitochondria in Cancer: Warburg and Beyond and Encouraging Prospects for Effective Therapies. Biochim Biophys Acta. 2010;1797(6–7):1225–30.

8. Palade GE. An electron microscope study of the mitochondrial structure. J Histochem Cytochem Off J Histochem Soc. 1953 Jul;1(4):188–211.

9. Frey TG, Mannella CA. The internal structure of mitochondria. Trends Biochem Sci. 2000 Jul;25(7):319–24.

10. Distler AM, Kerner J, Hoppel CL. Proteomics of mitochondrial inner and outer membranes. Proteomics. 2008 Oct;8(19):4066–82.

11. Westermann B. Mitochondrial fusion and fission in cell life and death. Nat Rev Mol Cell Biol. 2010 Dec 1;11(12):872–84.

12. Skulachev VP. Mitochondrial filaments and clusters as intracellular power-transmitting cables. Trends Biochem Sci. 2001 Jan;26(1):23–9.

13. Sesaki H, Jensen RE. Division versus fusion: Dnm1p and Fzo1p antagonistically regulate mitochondrial shape. J Cell Biol. 1999 Nov 15;147(4):699–706.

14. Sarzi E, Angebault C, Seveno M, Gueguen N, Chaix B, Bielicki G, et al. The human OPA1delTTAG mutation induces premature age-related systemic neurodegeneration in mouse. Brain. 2012 Dec 1;135(12):3599–613.

15. Korwitz A, Merkwirth C, Richter-Dennerlein R, Tröder SE, Sprenger H-G, Quirós PM, et al. Loss of OMA1 delays neurodegeneration by preventing stress-induced OPA1 processing in mitochondria. J Cell Biol. 2016 Jan 18;212(2):157–66.

16. Herlan M, Vogel F, Bornhovd C, Neupert W, Reichert AS. Processing of Mgm1 by the rhomboid-type protease Pcp1 is required for maintenance of mitochondrial morphology and of mitochondrial DNA. J Biol Chem. 2003 Jul 25;278(30):27781–8.

17. Galper JB. MITOCHONDRIAL PROTEIN SYNTHESIS IN HELA CELLS. J Cell Biol. 1974 Mar 1;60(3):755–63.

18. Eilers M, Schatz G. Binding of a specific ligand inhibits import of a purified precursor protein into mitochondria. Nature. 1986 Jul 17;322(6076):228–32.

19. Bioenergetics. Elsevier; 2011. 412 p.

20. Anderson S, Bankier AT, Barrell BG, de Bruijn MHL, Coulson AR, Drouin J, et al. Sequence and organization of the human mitochondrial genome. Nature. 1981 Apr 9;290(5806):457–65.

21. Replication of Circular DNA in Eukaryotic Cells. Annu Rev Biochem. 1974;43(1):695–719.

22. Taanman J-W. The mitochondrial genome: structure, transcription, translation and replication. Biochim Biophys Acta BBA - Bioenerg. 1999 Feb 9;1410(2):103–23.

23. Fontanesi F. Mitochondria: Structure and Role in Respiration. In: eLS [Internet]. John Wiley & Sons, Ltd; 2001 [cited 2017 Jan 18]. Available from: http://onlinelibrary.wiley.com/doi/10.1002/9780470015902.a0001380.pub2/abstract

24. Turrens JF. Mitochondrial formation of reactive oxygen species. J Physiol. 2003 Oct 15;552(Pt 2):335–44.

25. Cannon B, Nedergaard J. Brown adipose tissue: function and physiological significance. Physiol Rev. 2004 Jan;84(1):277–359.

26. Rich PR. The molecular machinery of Keilin's respiratory chain. Biochem Soc Trans. 2003 Dec;31(Pt 6):1095–105.

27. Mitchell P. Keilin's respiratory chain concept and its chemiosmotic consequences. Science. 1979 Dec 7;206(4423):1148–59.

28. Role of Mitochondrial Calcium Transport in the Control of Substrate Oxidation [Internet]. PubMed Journals. [cited 2017 Jan 19]. Available from: https://ncbi.nlm.nih.gov/labs/articles/9746330/

29. Adam-Vizi V, Chinopoulos C. Bioenergetics and the formation of mitochondrial reactive oxygen species. Trends Pharmacol Sci. 2006 Dec;27(12):639–45.

30. Bernardi P. Mitochondrial transport of cations: channels, exchangers, and permeability transition. Physiol Rev. 1999 Oct;79(4):1127–55.

31. Spinazzi M, Cazzola S, Bortolozzi M, Baracca A, Loro E, Casarin A, et al. A novel deletion in the GTPase domain of OPA1 causes defects in mitochondrial morphology and distribution, but not in function. Hum Mol Genet. 2008;17(21):3291–302.

32. I principi di biochimica di Lehninger - Zanichelli [Internet]. [cited 2017 Jan 19]. Available from: http://www.zanichelli.it/ricerca/prodotti/i-principi-di-biochimica-di-lehninger-nelson-cox

33. Walker JE. The ATP synthase: the understood, the uncertain and the unknown. Biochem Soc Trans. 2013 Feb 1;41(1):1–16.

34. Collinson IR, van Raaij MJ, Runswick MJ, Fearnley IM, Skehel JM, Orriss GL, et al. ATP synthase from bovine heart mitochondria. In vitro assembly of a stalk complex in the presence of F1-ATPase and in its absence. J Mol Biol. 1994 Sep 30;242(4):408–21.

35. Rees DM, Leslie AGW, Walker JE. The structure of the membrane extrinsic region of bovine ATP synthase. Proc Natl Acad Sci U S A. 2009 Dec 22;106(51):21597–601.

36. Boyer PD. The binding change mechanism for ATP synthase--some probabilities and possibilities. Biochim Biophys Acta. 1993 Jan 8;1140(3):215–50.

37. Harris DA, Das AM. Control of mitochondrial ATP synthesis in the heart. Biochem J. 1991 Dec 15;280(Pt 3):561–73.

38. Rouslin W. Regulation of the mitochondrial ATPase in situ in cardiac muscle: role of the inhibitor subunit. J Bioenerg Biomembr. 1991 Dec;23(6):873–88.

39. Leslie AG, Walker JE. Structural model of F1-ATPase and the implications for rotary catalysis. Philos Trans R Soc B Biol Sci. 2000 Apr 29;355(1396):465–71.

40. Strauss M, Hofhaus G, Schröder RR, Kühlbrandt W. Dimer ribbons of ATP synthase shape the inner mitochondrial membrane. EMBO J. 2008 Apr 9;27(7):1154–60.

41. Moreno-Sánchez R, Hogue BA, Hansford RG. Influence of NAD-linked dehydrogenase activity on flux through oxidative phosphorylation. Biochem J. 1990 Jun 1;268(2):421–8.

42. Pullman ME, Monroy GC. A Naturally Occurring Inhibitor of Mitochondrial Adenosine Triphosphatase. J Biol Chem. 1963 Nov 1;238(11):3762–9.

43. Cabezón E, Runswick MJ, Leslie AGW, Walker JE. The structure of bovine IF1, the regulatory subunit of mitochondrial F-ATPase. EMBO J. 2001 Dec 17;20(24):6990–6.

44. Green DW, Grover GJ. The IF(1) inhibitor protein of the mitochondrial F(1)F(0)-ATPase. Biochim Biophys Acta. 2000 May 31;1458(2–3):343–55.

45. Cabezón E, Arechaga I, Jonathan P, Butler G, Walker JE. Dimerization of Bovine F1-ATPase by Binding the Inhibitor Protein, IF1. J Biol Chem. 2000 Sep 15;275(37):28353–5.

46. Contessi S, Haraux F, Mavelli I, Lippe G. Identification of a conserved calmodulin-binding motif in the sequence of F0F1 ATPsynthase inhibitor protein. J Bioenerg Biomembr. 2005 Oct;37(5):317–26.

47. Faccenda D, Campanella M. Molecular Regulation of the Mitochondrial F1Fo-ATPsynthase: Physiological and Pathological Significance of the Inhibitory Factor 1 (IF 1). Int J Cell Biol. 2012 Aug 26;2012:e367934.

48. Gledhill JR, Montgomery MG, Leslie AGW, Walker JE. How the regulatory protein, IF(1), inhibits F(1)-ATPase from bovine mitochondria. Proc Natl Acad Sci U S A. 2007 Oct 2;104(40):15671–6.

49. Campanella M, Casswell E, Chong S, Farah Z, Wieckowski MR, Abramov AY, et al. Regulation of Mitochondrial Structure and Function by the F1Fo-ATPase Inhibitor Protein, IF1. Cell Metab. 2008 Jul;8(1):13–25.

50. Solaini G, Harris DA. Biochemical dysfunction in heart mitochondria exposed to ischaemia and reperfusion. Biochem J. 2005 Sep 1;390(Pt 2):377–94.

51. Sánchez-Cenizo L, Formentini L, Aldea M, Ortega AD, García-Huerta P, Sánchez-Aragó M, et al. Up-regulation of the ATPase inhibitory factor 1 (IF1) of the mitochondrial H+-ATP synthase in human tumors mediates the metabolic shift of cancer cells to a Warburg phenotype. J Biol Chem. 2010 Aug 13;285(33):25308–13.

52. Sánchez-Aragó M, Formentini L, Martínez-Reyes I, García-Bermudez J, Santacatterina F, Sánchez-Cenizo L, et al. Expression, regulation and clinical relevance of the ATPase inhibitory factor 1 in human cancers. Oncogenesis. 2013 Apr 22;2:e46.

53. Formentini L, Sánchez-Aragó M, Sánchez-Cenizo L, Cuezva JM. The mitochondrial ATPase inhibitory factor 1 triggers a ROS-mediated retrograde prosurvival and proliferative response. Mol Cell. 2012 Mar 30;45(6):731–42.

54. Matés JM, Sánchez-Jiménez FM. Role of reactive oxygen species in apoptosis: implications for cancer therapy. Int J Biochem Cell Biol. 2000 Feb;32(2):157–70.

55. Faccenda D, Tan CH, Duchen MR, Campanella M. Mitochondrial IF1 preserves cristae structure to limit apoptotic cell death signaling. Cell Cycle. 2013 Aug 15;12(16):2530–2.

56. Fujikawa M, Imamura H, Nakamura J, Yoshida M. Assessing actual contribution of IF1, inhibitor of mitochondrial FoF1, to ATP homeostasis, cell growth, mitochondrial morphology, and cell viability. J Biol Chem. 2012 May 25;287(22):18781–7.

57. Barbato S, Sgarbi G, Gorini G, Baracca A, Solaini G. The Inhibitor Protein (IF $_1$) of the F $_1$ F $_0$ -ATPase Modulates Human Osteosarcoma Cell Bioenergetics. J Biol Chem. 2015 Mar 6;290(10):6338–48.

58. García JJ, Morales-Ríos E, Cortés-Hernández P, Rodríguez-Zavala JS. The Inhibitor Protein (IF1) Promotes Dimerization of the Mitochondrial F1F0-ATP Synthase. Biochemistry (Mosc). 2006 Oct 1;45(42):12695–703.

59. Tomasetig L, Di Pancrazio F, Harris DA, Mavelli I, Lippe G. Dimerization of F0F1ATP synthase from bovine heart is independent from the binding of the inhibitor protein IF1. Biochim Biophys Acta. 2002 Dec 2;1556(2–3):133–41.

60. Vander Heiden MG, Cantley LC, Thompson CB. Understanding the Warburg effect: the metabolic requirements of cell proliferation. Science. 2009 May 22;324(5930):1029–33.

61. Cairns RA, Harris IS, Mak TW. Regulation of cancer cell metabolism. Nat Rev Cancer. 2011 Feb;11(2):85–95.

62. Warburg OH, Biologie K-W-I für. Über den Stoffwechsel der Tumoren. J. Springer; 1926. 276 p.

63. Gillies RJ, Gatenby RA. Adaptive landscapes and emergent phenotypes: why do cancers have high glycolysis? J Bioenerg Biomembr. 2007 Jun;39(3):251–7.

64. Herst PM, Berridge MV. Cell surface oxygen consumption: A major contributor to cellular oxygen consumption in glycolytic cancer cell lines. Biochim Biophys Acta BBA - Bioenerg. 2007 Feb;1767(2):170–7.

65. Rodríguez-Enríquez S, Vital-González PA, Flores-Rodríguez FL, Marín-Hernández A, Ruiz-Azuara L, Moreno-Sánchez R. Control of cellular proliferation by modulation of oxidative phosphorylation in human and rodent fast-growing tumor cells. Toxicol Appl Pharmacol. 2006 Sep 1;215(2):208–17.

66. Vaupel P, Kallinowski F, Okunieff P. Blood flow, oxygen and nutrient supply, and metabolic microenvironment of human tumors: a review. Cancer Res. 1989 Dec 1;49(23):6449–65.

67. Baronzio G, Freitas I, Kwaan HC. Tumor microenvironment and hemorheological abnormalities. Semin Thromb Hemost. 2003 Oct;29(5):489–97.

68. Semenza GL. Oxygen Sensing, Homeostasis, and Disease. N Engl J Med. 2011 Aug 11;365(6):537–47.

69. Kim J, Tchernyshyov I, Semenza GL, Dang CV. HIF-1-mediated expression of pyruvate dehydrogenase kinase: a metabolic switch required for cellular adaptation to hypoxia. Cell Metab. 2006 Mar;3(3):177–85.

70. Papandreou I, Cairns RA, Fontana L, Lim AL, Denko NC. HIF-1 mediates adaptation to hypoxia by actively downregulating mitochondrial oxygen consumption. Cell Metab. 2006 Mar;3(3):187–97.

71. Solaini G, Baracca A, Lenaz G, Sgarbi G. Hypoxia and mitochondrial oxidative metabolism. Biochim Biophys Acta. 2010 Jul;1797(6–7):1171–7.

72. Hinkle PC, Butow RA, Racker E, Chance B. Partial Resolution of the Enzymes Catalyzing Oxidative Phosphorylation XV. REVERSE ELECTRON TRANSFER IN THE FLAVIN-CYTOCHROME b REGION OF THE RESPIRATORY CHAIN OF BEEF HEART SUBMITOCHONDRIAL PARTICLES. J Biol Chem. 1967 Nov 25;242(22):5169–73.

73. Boveris A, Cadenas E. Mitochondrial production of superoxide anions and its relationship to the antimycin insensitive respiration. FEBS Lett. 1975 Jul 1;54(3):311–4.

74. Weisiger RA, Fridovich I. Mitochondrial superoxide simutase. Site of synthesis and intramitochondrial localization. J Biol Chem. 1973 Jul 10;248(13):4793–6.

75. Chandel NS, McClintock DS, Feliciano CE, Wood TM, Melendez JA, Rodriguez AM, et al. Reactive Oxygen Species Generated at Mitochondrial Complex III Stabilize Hypoxia-

inducible Factor-1α during Hypoxia A MECHANISM OF O2 SENSING. J Biol Chem. 2000 Aug 18;275(33):25130–8.

76. Han D, Williams E, Cadenas E. Mitochondrial respiratory chain-dependent generation of superoxide anion and its release into the intermembrane space. Biochem J. 2001 Jan 15;353(Pt 2):411–6.

77. Turrens JF. Mitochondrial formation of reactive oxygen species. J Physiol. 2003 Oct 15;552(Pt 2):335–44.

78. Vaux EC, Metzen E, Yeates KM, Ratcliffe PJ. Regulation of hypoxia-inducible factor is preserved in the absence of a functioning mitochondrial respiratory chain. Blood. 2001 Jul 15;98(2):296–302.

79. Semenza GL. Hypoxia and human disease-and the Journal of Molecular Medicine. J Mol Med Berl Ger. 2007 Dec;85(12):1293–4.

80. Waypa GB, Schumacker PT. O(2) sensing in hypoxic pulmonary vasoconstriction: the mitochondrial door re-opens. Respir Physiol Neurobiol. 2002 Aug 22;132(1):81–91.

81. Kovac S, Angelova PR, Holmström KM, Zhang Y, Dinkova-Kostova AT, Abramov AY. Nrf2 regulates ROS production by mitochondria and NADPH oxidase. Biochim Biophys Acta. 2015 Apr;1850(4):794–801.

82. Palmeira CM, Moreno AJM, editors. Mitochondrial bioenergetics: methods and protocols. New York: Humana Press; 2012. 333 p. (Methods in molecular biology).

83. Toppo S, Flohé L, Ursini F, Vanin S, Maiorino M. Catalytic mechanisms and specificities of glutathione peroxidases: variations of a basic scheme. Biochim Biophys Acta. 2009 Nov;1790(11):1486–500.

84. Marklund SL, Bjelle A, Elmqvist LG. Superoxide dismutase isoenzymes of the synovial fluid in rheumatoid arthritis and in reactive arthritides. Ann Rheum Dis. 1986 Oct;45(10):847–51.

85. Schroeder WA, Shelton JR, Shelton JB, Robberson B, Apell G, Fang RS, et al. The complete amino acid sequence of bovine liver catalase and the partial sequence of bovine erythrocyte catalase. Arch Biochem Biophys. 1982 Mar;214(1):397–421.

86. Agar NS, Sadrzadeh SM, Hallaway PE, Eaton JW. Erythrocyte catalase. A somatic oxidant defense? J Clin Invest. 1986 Jan;77(1):319–21.

87. Mizushima N, Komatsu M. Autophagy: renovation of cells and tissues. Cell. 2011 Nov 11;147(4):728–41.

88. Kim I, Rodriguez-Enriquez S, Lemasters JJ. Selective degradation of mitochondria by mitophagy. Arch Biochem Biophys. 2007 Jun 15;462(2):245–53.

89. Head B, Griparic L, Amiri M, Gandre-Babbe S, van der Bliek AM. Inducible proteolytic inactivation of OPA1 mediated by the OMA1 protease in mammalian cells. J Cell Biol. 2009 Dec 28;187(7):959–66.

90. Boland ML, Chourasia AH, Macleod KF. Mitochondrial dysfunction in cancer. Front Oncol. 2013 Dec 2;3:292.

91. Lefebvre V, Du Q, Baird S, Ng AC-H, Nascimento M, Campanella M, et al. Genome-wide RNAi screen identifies ATPase inhibitory factor 1 (ATPIF1) as essential for PARK2 recruitment and mitophagy. Autophagy. 2013 Nov 1;9(11):1770–9.

92. Salvesen GS, Dixit VM. Caspases: intracellular signaling by proteolysis. Cell. 1997 Nov 14;91(4):443–6.

93. Locksley RM, Killeen N, Lenardo MJ. The TNF and TNF receptor superfamilies: integrating mammalian biology. Cell. 2001 Feb 23;104(4):487–501.

94. Kuida K. Caspase-9. Int J Biochem Cell Biol. 2000 Feb;32(2):121–4.

95. Cory S, Adams JM. The Bcl2 family: regulators of the cellular life-or-death switch. Nat Rev Cancer. 2002 Sep;2(9):647–56.

96. Galluzzi L, Kroemer G. Mitochondrial apoptosis without VDAC. Nat Cell Biol. 2007 May;9(5):487–9.

97. Vaux DL, Cory S, Adams JM. Bcl-2 gene promotes haemopoietic cell survival and cooperates with c-myc to immortalize pre-B cells. Nature. 1988 Sep 29;335(6189):440–2.

98. Clapham DE. Calcium Signaling. Cell. 2007 Dec 14;131(6):1047–58.

99. Bootman MD, Berridge MJ, Roderick HL. Calcium signalling: more messengers, more channels, more complexity. Curr Biol CB. 2002 Aug 20;12(16):R563-565.

100. Kelley GG, Reks SE, Ondrako JM, Smrcka AV. Phospholipase C(epsilon): a novel Ras effector. EMBO J. 2001 Feb 15;20(4):743–54.

101. Ishii K, Hirose K, Iino M. Ca2+ shuttling between endoplasmic reticulum and mitochondria underlying Ca2+ oscillations. EMBO Rep. 2006 Apr;7(4):390–6.

102. Aguilar-Maldonado B, Gómez-Viquez L, García L, Del Angel RM, Arias-Montaño JA, Guerrero-Hernández A. Histamine potentiates IP3-mediated Ca2+ release via thapsigargin-sensitive Ca2+ pumps. Cell Signal. 2003 Jul;15(7):689–97.

103. Rizzuto R, Pinton P, Carrington W, Fay FS, Fogarty KE, Lifshitz LM, et al. Close Contacts with the Endoplasmic Reticulum as Determinants of Mitochondrial Ca2+ Responses. Science. 1998 Jun 12;280(5370):1763–6.

104. Gatliff J, Campanella M. The 18 kDa translocator protein (TSPO): a new perspective in mitochondrial biology. Curr Mol Med. 2012 May;12(4):356–68.

105. Gincel D, Zaid H, Shoshan-Barmatz V. Calcium binding and translocation by the voltage-dependent anion channel: a possible regulatory mechanism in mitochondrial function. Biochem J. 2001 Aug 15;358(Pt 1):147–55.

106. Patron M, Raffaello A, Granatiero V, Tosatto A, Merli G, De Stefani D, et al. The mitochondrial calcium uniporter (MCU): molecular identity and physiological roles. J Biol Chem. 2013 Apr 12;288(15):10750–8.

107. Mallilankaraman K, Doonan P, Cárdenas C, Chandramoorthy HC, Müller M, Miller R, et al. MICU1 is an essential gatekeeper for MCU-mediated mitochondrial Ca(2+) uptake that regulates cell survival. Cell. 2012 Oct 26;151(3):630–44.

108. Csordás G, Golenár T, Seifert EL, Kamer KJ, Sancak Y, Perocchi F, et al. MICU1 controls both the threshold and cooperative activation of the mitochondrial Ca^{2+} uniporter. Cell Metab. 2013 Jun 4;17(6):976–87.

109. Shanmughapriya S, Rajan S, Hoffman NE, Zhang X, Guo S, Kolesar JE, et al. Ca2+ signals regulate mitochondrial metabolism by stimulating CREB-mediated expression of the mitochondrial Ca2+ uniporter gene mcu. Sci Signal. 2015 Mar 3;8(366):ra23.

110. Denton RM. Regulation of mitochondrial dehydrogenases by calcium ions. Biochim Biophys Acta. 2009 Nov;1787(11):1309–16.

111. Turkan A, Hiromasa Y, Roche TE. Formation of a complex of the catalytic subunit of pyruvate dehydrogenase phosphatase isoform 1 (PDP1c) and the L2 domain forms a Ca2+ binding site and captures PDP1c as a monomer. Biochemistry (Mosc). 2004 Nov 30;43(47):15073–85.

112. Hubbard MJ, McHugh NJ. Mitochondrial ATP synthase F1-beta-subunit is a calcium-binding protein. FEBS Lett. 1996 Aug 12;391(3):323–9.

113. Boerries M, Most P, Gledhill JR, Walker JE, Katus HA, Koch WJ, et al. Ca2+ -dependent interaction of S100A1 with F1-ATPase leads to an increased ATP content in cardiomyocytes. Mol Cell Biol. 2007 Jun;27(12):4365–73.

114. Tarasov AI, Griffiths EJ, Rutter GA. Regulation of ATP production by mitochondrial Ca2+. Cell Calcium. 2012 Jul;52(1):28–35.

115. Rasola A, Bernardi P. Mitochondrial permeability transition in Ca(2+)-dependent apoptosis and necrosis. Cell Calcium. 2011 Sep;50(3):222–33.

116. Husain RSA, Ramakrishnan V. Global Variation of Human Papillomavirus Genotypes and Selected Genes Involved in Cervical Malignancies. Ann Glob Health. 2015 Sep;81(5):675–83.

117. Eifel PJ. Chemoradiotherapy in the treatment of cervical cancer. Semin Radiat Oncol. 2006 Jul;16(3):177–85.

118. Zielinski S. Henrietta Lacks' "Immortal" Cells [Internet]. Smithsonian. [cited 2017 Mar 3]. Available from: http://www.smithsonianmag.com/science-nature/henrietta-lacks-immortal-cells-6421299/

119. Scherer WF, Syverton JT, Gey GO. STUDIES ON THE PROPAGATION IN VITRO OF POLIOMYELITIS VIRUSES. J Exp Med. 1953 May 1;97(5):695–710.

120. PosthumaDeBoer J, Witlox MA, Kaspers GJL, van Royen BJ. Molecular alterations as target for therapy in metastatic osteosarcoma: a review of literature. Clin Exp Metastasis. 2011 Jun;28(5):493–503.

121. Vigorita VJ. Orthopaedic Pathology. Lippincott Williams & Wilkins; 2008. 816 p.

122. Broadhead ML, Clark JCM, Myers DE, Dass CR, Choong PFM. The Molecular Pathogenesis of Osteosarcoma: A Review. Sarcoma. 2011 Apr 13;2011:e959248.

123. Teodoro JG, Evans SK, Green MR. Inhibition of tumor angiogenesis by p53: a new role for the guardian of the genome. J Mol Med Berl Ger. 2007 Nov;85(11):1175–86.

124. Marina N, Gebhardt M, Teot L, Gorlick R. Biology and therapeutic advances for pediatric osteosarcoma. The Oncologist. 2004;9(4):422–41.

125. Shimizu T, Ishikawa T, Sugihara E, Kuninaka S, Miyamoto T, Mabuchi Y, et al. c-MYC overexpression with loss of Ink4a/Arf transforms bone marrow stromal cells into osteosarcoma accompanied by loss of adipogenesis. Oncogene. 2010 Oct 21;29(42):5687–99.

126. Hicklin DJ, Ellis LM. Role of the vascular endothelial growth factor pathway in tumor growth and angiogenesis. J Clin Oncol Off J Am Soc Clin Oncol. 2005 Feb 10;23(5):1011–27.

127. Zerbetto E, Vergani L, Dabbeni-Sala F. Quantification of muscle mitochondrial oxidative phosphorylation enzymes via histochemical staining of blue native polyacrylamide gels. Electrophoresis. 1997 Oct;18(11):2059–64.

128. Baracca A, Chiaradonna F, Sgarbi G, Solaini G, Alberghina L, Lenaz G. Mitochondrial Complex I decrease is responsible for bioenergetic dysfunction in K-ras transformed cells. Biochim Biophys Acta BBA - Bioenerg. 2010 Feb;1797(2):314–23.

129. Sgarbi G, Matarrese P, Pinti M, Lanzarini C, Ascione B, Gibellini L, et al. Mitochondria hyperfusion and elevated autophagic activity are key mechanisms for cellular bioenergetic preservation in centenarians. Aging. 2014 Apr 30;6(4):296–310.

130. Borsi E, Perrone G, Terragna C, Martello M, Dico AF, Solaini G, et al. Hypoxia inducible factor-1 alpha as a therapeutic target in multiple myeloma. Oncotarget. 2014 Apr 15;5(7):1779–92.

131. Hill JM, De Stefani D, Jones AWE, Ruiz A, Rizzuto R, Szabadkai G. Measuring Baseline Ca2+ Levels in Subcellular Compartments Using Genetically Engineered Fluorescent Indicators. Galluzzi L, Kroemer G, editors. CELL-WIDE Metab Alter Assoc Malig. 2014 Jan 1;543:47–72.

132. Lowry OH, Rosebrough NJ, Farr AL, Randall RJ, others. Protein measurement with the Folin phenol reagent. J Biol Chem. 1951;193(1):265–275.

133. Cabezon E, Butler PJ, Runswick MJ, Walker JE. Modulation of the oligomerization state of the bovine F1-ATPase inhibitor protein, IF1, by pH. J Biol Chem. 2000 Aug 18;275(33):25460–4.

134. Wittig I, Braun H-P, Schagger H. Blue native PAGE : Abstract : Nature Protocols. Nat Protoc. 2006 Jun;1(1):418–28.

135. Ichikawa N, Ushida S, Kawabata M, Masazumi Y. Nucleotide sequence of cDNA coding the mitochondrial precursor protein of the ATPase inhibitor from humans. Biosci Biotechnol Biochem. 1999 Dec;63(12):2225–7.

136. Porcelli AM, Angelin A, Ghelli A, Mariani E, Martinuzzi A, Carelli V, et al. Respiratory complex I dysfunction due to mitochondrial DNA mutations shifts the voltage threshold for opening of the permeability transition pore toward resting levels. J Biol Chem. 2009 Jan 23;284(4):2045–52.